



Cite this: *J. Mater. Chem. B*, 2021,  
9, 7076

## Recent near-infrared light-activated nanomedicine toward precision cancer therapy

Xiaowei Luan,<sup>†</sup> Yongchun Pan,<sup>†</sup> Yanfeng Gao and Yujun Song \*

Light has been present throughout the history of mankind and even the universe. It is of great significance to human life, contributing to energy, agriculture, communication, and much more. In the biomedical field, light has been developed as a switch to control medical processes with minimal invasion and high spatiotemporal selectivity. During the past three years, near-infrared (NIR) light as long-wavelength light has been applied to more than 3000 achievements in biological applications due to its deep penetration depth and low phototoxicity. Remotely controlled cancer therapy usually involves the conversion of biologically inert NIR light. Thus, various materials, especially nanomaterials that can generate reactive oxygen species (ROS), ultraviolet (UV)/visual light, or thermal energy and so on under NIR illumination achieve great potential for the research of nanomedicine. Here, we offered an overview of recent advances in NIR light-activated nanomedicine for cancer therapeutic applications. NIR-light-conversion nanotechnologies for both directly triggering nanodrugs and smart drug delivery toward tumor therapy were discussed emphatically. The challenges and future trends of the use of NIR light in biomedical applications were also provided as a conclusion. We expect that this review will spark inspiration for biologists, materials scientists, pharmacologists, and chemists to fight against diseases and boost the future clinical-translational applications of NIR technology-based precision nanomedicine.

Received 27th March 2021,  
Accepted 13th May 2021

DOI: 10.1039/d1tb00671a

rsc.li/materials-b

### 1. Introduction

What is the significance of light? It is supposed to hold the key, not only to the multiplication of life but even to the beginning

*College of Engineering and Applied Sciences, State Key Laboratory of Analytical Chemistry for Life Science, Collaborative Innovation Center of Advanced Nanostructures, Nanjing University, Nanjing, 210023, China.*  
E-mail: ysong@nju.edu.cn

<sup>†</sup> These authors contributed equally to this work and should be considered cofirst authors.

of the universe. In human life, light serves as an essential element, contributing to energy, agriculture, communication, and much more.<sup>1</sup> Over the past few decades, optical manipulation also ignited greater interest for applications in the medical field including local diagnosis, *in vivo* imaging, and phototherapy due to its minimal invasion and high spatiotemporal selectivity.<sup>2–6</sup> In particular, the exploration of near-infrared (NIR) light in biological applications is gaining strong momentum, and more than 3000 achievements regarding NIR phototherapy were found in the past three years (Fig. 1A). Generally speaking, biological tissue is



Xiaowei Luan

Xiaowei Luan is currently a PhD student under the supervision of Prof. Yujun Song at the College of Engineering and Applied Sciences, Nanjing University. She received her bachelor's degree (2017) and master's degree (2020) from Nanjing University. Her current research focuses on bioassays, genome editing, and cancer therapy.



Yongchun Pan

Yongchun Pan is currently a PhD candidate under Prof. Yujun Song at Nanjing University. He received his BS degree (2016) from Jiangnan University and then obtained his MA degree (2019) from Xiamen University under the supervision of Prof. Youhui Lin. His current research focuses on CRISPR-based nanomedicine and biosensors.



Fig. 1 (A) Number of publications retrieved from Web of Science on the topics of NIR and therapy; (B) schematic representation of NIR light excitation in direct therapy and on-demand delivery via generation of ROS, UV/visual light utilization, and heat production.

transparent to NIR light, which means that it is hardly utilized by living organisms directly, and thereby NIR light needs to be transformed into other available forms of energy with the aid of photosensitizers (PSs).<sup>7–9</sup> According to the energy forms directly generated from light, the strategies exploited thus far can be roughly classified into three categories, including (1) near-infrared induced reactive oxygen species (ROS)-based therapy, which is based on PSs (for example, porphyrin derivatives) to directly transform NIR energy into ROS generation for cell apoptosis; (2) near-infrared upconversion activated chemotherapy, where PSs would emit ultraviolet (UV)/visual light with a high energy to trigger not only ROS generation but various photochemical reactions under NIR irradiation; and (3) near-infrared photothermal cancer therapy achieved using light-heat conversion materials.

As an interdisciplinary science involving engineering, materials science, chemistry, biology, and medical science, nanomedicine, a branch of nanotechnology applied in health and medicine, can be traced back to the late 1990s and was first found in research publications in 2000.<sup>10,11</sup> The past two decades witnessed the rapidly growing influence of nanomedicine on healthcare, which pioneered a new route to therapeutics, *in vitro* diagnostics, and medical devices.<sup>12–15</sup> As stimuli-responsive nanomaterials progress,

nanomedicine obtains greater potential in clinical applications, and is presented with diversity, intelligence, and personalization.<sup>16</sup> Recent studies are intended to achieve smarter nanoplatforms for precision therapy which is triggered by easily available or location-specific signal sources.<sup>17–20</sup> Specific endogenous stimuli can be applied to enhance the ability of targeting treatment, such as acidity ( $H^+$ ), glutathione (GSH), and overexpression of certain enzymes in tumor cells (for example, cathepsin B).<sup>21–23</sup> Such stimuli-responsive nanoplatforms offer a possibility to deliver drugs in a spatially controlled fashion, but are indeed difficult for temporal control. Additionally, the patient individual difference in the expression of the markers increases the difficulty in the design of nanocarriers.<sup>24</sup> Compared with the endogenous counterparts, extracorporeal physical stimuli can be readily employed as switches for spatiotemporally controlled nanovehicles, from this point of view, which seems to be more promising. Of these stimuli, thermo-mediated treatment is among the most studied stimuli-responsive approaches, which is usually dominated by nanocarriers composed of at least one component that undergoes a nonlinear sharp change with temperature changes.<sup>25</sup> However, such thermo-responsive nanodevices were hampered by the difficult design of materials with both biocompatibility and high sensitivity to slight temperature fluctuations at the physiological temperature of about 37 °C, and the external heat source hardly gets directly to tumors deep inside without causing damage to the surrounding tissues. Magnetic guidance provides a spatiotemporally controllable strategy for cancer therapy, which was achieved by focusing a magnetic field on the required location after injecting a magnetically responsive nanoparticle, for example,  $Fe_3O_4$ .<sup>26</sup> This strategy has demonstrated huge potential in experimental tumor treatment due to enhanced accumulation of nanoparticles inside solid-tumor models. However, this method suffers from the complexity of constructing an external magnetic field to guarantee an adequate strength at deep penetration into the tissues. Currently, ultrasound (US) and light-mediated nanomedicines seem to be more promising candidates for spatiotemporal control over drugs due to their



Yanfeng Gao

Yanfeng Gao completed his PhD in Federal University of Toulouse-Midi-Pyrénées in 2018, focusing on inertial microfluidics. In 2019, he joined Nanjing University and is currently an Assistant Professor in the College of Engineering and Applied Sciences. His current research focuses on single-cell analysis, molecular recognition, genome editing and microfluidics.



Yujun Song

Yujun Song is currently a professor at the College of Engineering and Applied Sciences, Nanjing University. He received his BS degree from Wuhan University in 2005 and his PhD degree from Changchun Institute of Applied Chemistry, Chinese Academy of Sciences (CAS) in 2011. He then worked as a postdoctoral researcher at Houston Methodist hospital, Weill Cornell Medical College (USA) from 2011 to 2015. In early 2016, he joined Nanjing University. His current research is focused on biofunctional materials and microfluidics for translational medicine.

simple operation and high resolution.<sup>27,28</sup> In particular, NIR light-activated nanomedicine was more appealing for precision medicine as it overcomes the drawbacks of conventional nanosensitizers as well as the low tissue penetration depth and high phototoxicity with short-wavelength light.<sup>4,5,29</sup>

Here, we offered an overview of recent advances in NIR light-activated nanomedicine for cancer therapeutic applications. Since NIR light can readily propagate in human tissue without absorption, it needs to be transformed into other available forms to take effect, such as ROS, UV light, or thermal energy. The following discussions focus on NIR-light-converting nanotechnologies for both directly triggering nanodrugs and smart drug delivery toward tumor therapy (Fig. 1B). The challenges and future trends of the development of NIR light in biomedical applications<sup>30</sup> will be provided as a conclusion. We expect that this review will spark inspiration for biologists, material scientists, pharmacologists, and chemists to fight against diseases, and boost the future clinical-translational applications of NIR technology-based precision nanomedicine.

## 2. Near-infrared induced reactive oxygen species (ROS)-based nanomedicine

Reactive oxygen species (ROS) bear various physiological functions in organisms as well as damage cells.<sup>13</sup> Under NIR illumination, some PSs can result in the generation of ROS and subsequent damage to various organelles or drug nanocapsules. To augment the anticancer efficacy of NIR phototriggered platforms, recent advances are devoted to ROS evaluation *in vivo* and new-generation PSs with high conversion efficiencies.<sup>13</sup> In this section, we will highlight the issues and solutions to enhance near-infrared photodynamic therapy (NPDT), as well as the application of NIR-to-ROS conversion in targeted delivery.

### 2.1 Recent strategies to near-infrared photodynamic therapy (NPDT)

Photodynamic therapy (PDT) describes a noninvasive clinical modality with minimal toxicity for killing cancer cells through the increase of the local cytotoxic ROS level. However, the shallow penetration depth of short-wavelength excitation light hampers its application prospects and clinical value, and thus the employment of near-infrared light as a trigger for PDT seems to be urgent and promising.

According to the different photoreaction pathways of ROS generation, PDT can be classified as Type I and Type II (Fig. 2).<sup>31,32</sup> The former features the formation of radical species superoxide anions ( $\bullet\text{O}_2^-$ ), hydrogen peroxide ( $\text{H}_2\text{O}_2$ ), and hydroxyl radicals ( $\bullet\text{OH}$ ) *via*  $T_1$ -involving hydrogen- or electron-transfer processes, while the latter yields cytotoxic singlet oxygen ( $^1\text{O}_2$ ) resulting from the surrounding  $^3\text{O}_2$  through direct energy transfer. Among these ROS,  $\bullet\text{HO}$  with high oxidation capability towards almost all biological molecules could be generated by the Haber-Weiss/Fenton and disproportionation reactions of  $\bullet\text{O}_2$  with the assistance of the excited PS ( $T_1$ ) with no participation of oxygen.<sup>33,34</sup>

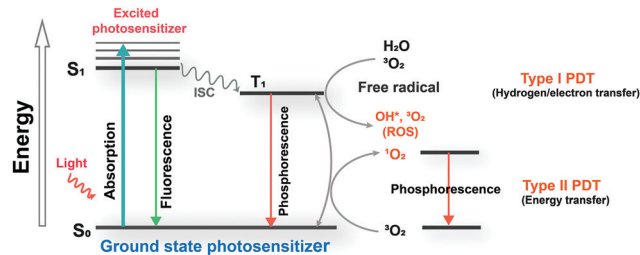


Fig. 2 Schematic representation of photochemical processes for different types of PDT.

Therefore, Type I PDT is regarded as a promising hypoxia strategy for cancer treatment.<sup>35–37</sup> However, relatively few Type I-associated PSs were reported and Type II PDT is commonly used currently.<sup>38</sup>

Light endows PDT with high spatiotemporal selectivity. Nevertheless, visible light for photoexcitation often suffers from its limited penetration depth ( $<1$  mm) owing to the strong absorption by most tissue.<sup>39,40</sup> One strategy to circumvent the drawback is to develop PSs which are excited by light in the NIR window. The excavation of NIR can avoid high energy (*i.e.*, UV or visible light) induced phototoxicity to healthy tissues.<sup>29</sup> Consequently, NPDT gradually becomes the mainstream as a versatile, flexible, and minimally invasive modulation of cancer therapeutics at underlying tissue.

The limited tissue penetration of light, the intrinsic hypoxic microenvironment of tumors, and the relatively low photon utilization efficiency of PSs constituted the main barriers to the clinical utility of PDT.<sup>41</sup> Implementation of NIR light, especially, the second NIR (NIR-II) light (1000 to 1700 nm) with further reduced interaction with tissues, to a large extent, has overcome the first problem. Hence, we summarize strategies to enhance the  $\text{O}_2$  level and the rational design of PSs for improving NPDT in the following discussion.

**2.1.1 *In situ* catalysis.** Compared with normal tissue cells, cancerous counterparts typically show a higher  $\text{H}_2\text{O}_2$  level due to their abnormal proliferation, apoptosis resistance, metastasis, and angiogenesis.<sup>42,43</sup> Inspired by the high  $\text{H}_2\text{O}_2$  level, researchers have developed a novel strategy for hypoxia alleviation by catalyzing the conversion of endogenous  $\text{H}_2\text{O}_2$  into  $\text{O}_2$ .<sup>44–53</sup> Chen *et al.* developed catalase (CAT) and human serum albumin (HSA)-comodified gold nanoclusters (AuNCs) as an  $\text{O}_2$  self-sufficient nanoplatform for PDT.<sup>54</sup> After intravenous injection, the CAT in the nanoparticles catalyzed the decomposition of  $\text{H}_2\text{O}_2$  to facilitate hypoxic-tumor photodynamic therapy under NIR-II light (1064 nm) irradiation in the domain of cancerization. For further improving the intracellular  $\text{O}_2$ -supply pathway, glucose oxidase (GOx) was introduced to accelerate the glucose consumption and  $\text{H}_2\text{O}_2$  generation. This strategy brings an additional benefit, that is, exhausted glucose would cut the energy supply and affect cancer cell proliferation and metabolism, and thus higher therapeutic effects would be achieved. Additionally, Li *et al.* embedded GOx and catalase in a cancer cell membrane which was coated on a porphyrin MOF (designated as mCGP). Due to the biomimetic surface functionalization, the obtained mCGPs



**Fig. 3** Strategies to enhance NPDT. (A) Schematic illustration of nanozyme-based cascade reactions for ROS generation to induce cell death; reproduced with permission from ref. 60. Copyright 2020 Elsevier Inc. (B) TH588-inhibiting MTH1 for PDT enhancement and the expression of apoptosis signaling protein identified by western blot analysis; reproduced with permission from ref. 72. Copyright 2020 American Association for the Advancement of Science. (C) Remodeling extracellular matrix; reproduced with permission from ref. 75. Copyright 2020 Elsevier Inc. (D) Design of light-responsive <sup>1</sup>O<sub>2</sub> capture and release for therapy; reproduced with permission from ref. 86. Copyright 2020 Wiley-VCH.

improved retention abilities and cancer targeting.<sup>55</sup> After accumulating at the tumor site, mCGPs could lead to a higher O<sub>2</sub> level by catalyzing the endogenous H<sub>2</sub>O<sub>2</sub>, and subsequently such O<sub>2</sub> was applied for intracellular glucose depletion and the increase of H<sub>2</sub>O<sub>2</sub>. Once the NIR light was turned on, <sup>1</sup>O<sub>2</sub> was continuously generated and assisted an amplified combined therapeutic effect, providing efficient inhibition of cancer growth in mice.

Plenty of nanomaterials have been discovered having enzyme-like activities including catalase mimics, glucose oxidase (GOx)-mimicking activities, and superoxide dismutase (SOD) mimics, that is, nanozymes, with low cost and high operational stability, being an ideal candidate for natural enzymes.<sup>56–59</sup> Our group recently proposed an NIR light-enhanced cascade nanozyme to fight against the hypoxic environment by using AuNP doped iron-based metal–organic frameworks (MOFs).<sup>60</sup> In this system, an iron-based MOF was employed to protect the GOx-like activity of AuNPs from protein-induced surface passivation and catalyze H<sub>2</sub>O<sub>2</sub> into O<sub>2</sub> and •OH (Fig. 3A). The results displayed that the activity of AuNPs can be enhanced under NIR monitoring, leading to a high H<sub>2</sub>O<sub>2</sub> level, which dramatically promoted the ROS generation by Fenton reaction for tumor suppression.

**2.1.2 Regulation of signaling pathways.** The high expression of reducing substances (*i.e.* GSH) in cancer cells would reduce O<sub>2</sub> and scavenge cellular ROS, which exacerbate the hypoxia of solid tumors and weaken the PDT.<sup>61–63</sup> To date, several attempts to lower the level of such substances were reported; in particular, Mn-based nanomaterials, the common GSH-consumption agents, provided an effective strategy for enhancing NPDT.<sup>64–67</sup> Alternatively, several signaling pathways involving intracellular oxidation or reduction also contributed to relieving hypoxia.<sup>35,68–72</sup> For instance, cutting off the expression of MTH1 can lead to ROS-economy by reducing the application of ROS for the hydrolysis and phosphorylation of 8-oxo-dG.<sup>72</sup> In this case,

TH588 (an inhibitor to MTH1) and chlorine e6 (Ce6) were concomitantly delivered by silica cross-linked micelles (SCLMs) for the satisfactory therapeutic effect of combined PDT and chemotherapy (CHT). To investigate the mechanism of this synergistic therapy, the authors examined the protein expression in the apoptosis signaling pathway, and the results suggested that the up-regulation of p53 was relevant to the apoptosis of cancer cells (Fig. 3B). As another ROS-defense system, the oxidative phosphorylation (OXPHOS) metabolic pathway was detrimental to PDT by consuming ROS as well,<sup>35</sup> and thus the  $\pi$ - $\pi$  stacking based nanoassembly of chlorine e6 (Ce6, a photosensitizer) and atovaquone (ATO, an OXPHOS inhibitor) achieved enhanced PDT.<sup>73</sup> After being injected intravenously, the nanoassemblies with a proper size exhibited preferential tumor accumulation *via* the enhanced permeability and retention (EPR) effect. As ATO interrupted the mitochondrial electron transport chain (ETC) of the mitochondrial complexes, the O<sub>2</sub> consumption of OXPHOS was hindered, and thereby the hypoxic microenvironment was relieved for augmenting PDT efficiency with low systemic toxicity.

As a common transcription factor in solid tumor, hypoxia-inducible factor 1 $\alpha$  (HIF-1 $\alpha$ ) is sensitive to the available oxygen in cells.<sup>74</sup> Typically, the intrinsic hypoxic tumor microenvironment can promote the expression of HIF-1 $\alpha$ , and thereby researchers are curious about whether the inhibition of HIF-1 can conversely improve the hypoxic microenvironment and be beneficial for PDT. A number of research studies have been performed and provided positive findings.<sup>69–71</sup> For example, Pan *et al.* constructed programmable DNA nanosponges for enhancing the efficacy of PDT using rolling circle amplification (RCA).<sup>70</sup> The nanosponges encoded *HIF-1 $\alpha$*  antisense DNA for the regulation of HIF-1 and downstream survival signaling, loaded PS for PDT, and included catalase to trigger O<sub>2</sub> generation. In view of the experimental results, their findings demonstrated the robust anticancer efficacy of PDT with remarkable biosafety both *in vitro* and *in vivo*.

**2.1.3 Remodeling the extracellular matrix.** Very recently, an anti-fibrotic drug was applied for the down-regulation of the components (*i.e.* hyaluronic acid (HA) and collagen I) in the tumor extracellular matrix (ECM) to relieve the hypoxic state in solid tumors.<sup>75</sup> In a study by Zhang's group, they loaded the drug (pirfenidone, PFD) in a poly(lactic-*co*-glycolic-acid)-poly(ethylene glycol) (PLGA-PEG) coated functional covalent organic framework (COF). After intravenous administration, PFD could be released from the COF at the tumor site, reducing ECM components and the intertumoral solid stress (Fig. 3C). Besides, this strategy was also conducive to blood vessel depressurization and vascular functional remodeling for higher oxygen supply in the tumor. Therefore, the subsequent injection of a micelle based protoporphyrin IX (PPIX)-conjugated peptide could achieve higher ROS generation and an enhanced NPDT effect in the alleviated tumor microenvironment *in vivo*.

**2.1.4 Sophisticated photosensitizers.** The antitumor effect of NPDT is strongly associated with the PS, and thus the rational design of an ingenious PS with high photon utilization efficiency but low systemic toxicity seemed to be urgent. Recently, Zhao *et al.* synthesized a smart organic molecule (Icy-NBF) containing

nitrobenzene moieties as a switchable PS for enhanced NPDT.<sup>76</sup> When reaching the hypoxic environment where nitroreductase (NTR) was overexpressed, Icy-NBF can be converted into Icy-NH<sub>2</sub> due to the reduction of nitrobenzene. The research found that Icy-NH<sub>2</sub> demonstrated a different excited state deactivation pathway, that is, Icy-NBF can produce effective <sup>1</sup>O<sub>2</sub> under 808 nm laser irradiation, while Icy-NH<sub>2</sub> converted light into heat. This interesting phenomenon implied that the obtained PSs improved the photon utilization and can be switched between photodynamic and photothermal agents by oxygen concentration for efficient tumor photoablation. Besides, plenty of inorganic materials were developed to generate ROS under NIR irradiation, which offered more PS alternatives for NPDT.<sup>77–81</sup> For example, an atomic-level ring-shaped MoOx (termed atomic-level nanorings, A-NRs) has been applied for NIR-phototherapy as a promising PS as well as a photothermal agent.<sup>79</sup> Besides, an interesting Z-scheme SnS<sub>1.68</sub>-WO<sub>2.41</sub> nanoplatform was developed for antitumor therapy.<sup>82</sup> Under NIR light, the nanocatalyst can achieve oxidative holes and hydrogen molecules, leading to ROS enhancement and hydrogen therapy. Both the *in vitro* and *in vivo* experiments displayed that the nanocatalyst performed well in inducing apoptosis.

Semiconducting polymers with special optical responses have been extensively developed for biomedical applications recently.<sup>83–85</sup> In an interesting study, a semiconducting polymer (pyrrolopyrrolidone-tetraphenylethylene, DPPTPE) and a 2-pyridone-based amphiphilic diblock polymer (PEG-Py) were mixed to prepare a kind of highly efficient PS (DPPTPE@PEG-Py NP).<sup>86</sup> In a previous report, the 2-pyridone group reacting with <sup>1</sup>O<sub>2</sub> could result in endoperoxides of 2-pyridone, which in turn could release <sup>1</sup>O<sub>2</sub> after thermal cycloreversion *in vivo*. Thus, DPPTPE@PEG-Py NPs could harvest <sup>1</sup>O<sub>2</sub> from DPPTPE under irradiation and transform it into PEG-Py. When the O<sub>2</sub> supply is insufficient (such as in the hypoxic tumor microenvironment), the chemical storage of <sup>1</sup>O<sub>2</sub> was released even in dark cycles (Fig. 3D). What is more, the DPPTPE@PEG-Py NP also can act as a photothermal agent, leading to synergistic PTT/PDT.

The rational design of nanocarriers can lower the systemic toxicity as well.<sup>87,88</sup> In a work by Liu and his co-workers, PSs (coumarin and Nile Blue) were covalently linked to the PEO skeleton for a NAD(P)H:quinone oxidoreductase isozyme 1 (NQO1, an enzyme related to many types of tumors)-responsive multifunctional polymeric vesicle.<sup>88</sup> In cells with low or no NQO1, PSs remained in the “off” state on account of the aggregation-induced quenching and quinone-rendered quenching resulting from photoinduced electron transfer (PET). Once the vesicle was internalized into the target tumor, intracellular NQO1 could actuate the self-immolative cleavage of the quinone trimethyl group and release PSs for PDT activation. After being conjugated with the DOTA-Gd complex, the vesicle was endowed with magnetic resonance (MR) imaging when the NQO1-induced shape transformation occurred.

## 2.2 Phototriggered ROS-targeted delivery

The nonspecific release of traditional drug carriers hardly maximized the anticancer effect, and therefore exploring stimuli-responsive materials for the design of site-specific delivery seemed to be promising.<sup>89</sup> Among various stimuli, the emergence of NIR

phototriggered ROS-mediated methods demonstrated great potential in virtue of their flexibility and simplicity of manipulation. Generally, ROS-sensitive materials involve two mechanisms: (1) the breakage of chemical bonds and (2) the change of hydrophobicity.<sup>90</sup> For the former, arylboronic ester, dithioketal, dialkoxy anthracene, and vinylidithio ether derivatives, which would be cleaved by ROS oxidation, are commonly used as linkers for on-demand delivery.<sup>91–100</sup> For example, based on an arylboronic ester, Xu's group has designed an ROS-sensitive cyclodextrin derivative to encapsulate DOX and a photosensitizer (purpurin 18).<sup>99</sup> Besides the ROS in the tumor microenvironment, NIR laser illumination also contributed to the release of DOX owing to the ROS generation from purpurin 18 upon NIR illumination. In 2019, NIR light controlled CRISPR/Cas9 delivery based on dithioketal was designed by Pu's group for precise gene editing.<sup>92</sup> When the NIR light was turned on, modified semiconducting polymer nanomaterials (SPNs) could produce <sup>1</sup>O<sub>2</sub> for the breakage of the dithioketal moiety and the subsequent dissociation of modified brushes to release Cas9 (Fig. 4A–C). Liposomes also underwent disassembly by such photooxidation for drug delivery, which was developed by You's group.<sup>101</sup> They have ever loaded ICG-ODA (a PS used for optical imaging) and doxorubicin (DOX) in a human epidermal growth factor receptor-2 (Her2) antibody-inserting liposome. After NIR irradiation, the amount of ROS increased and thereby damaged the nanostructure, resulting in the release

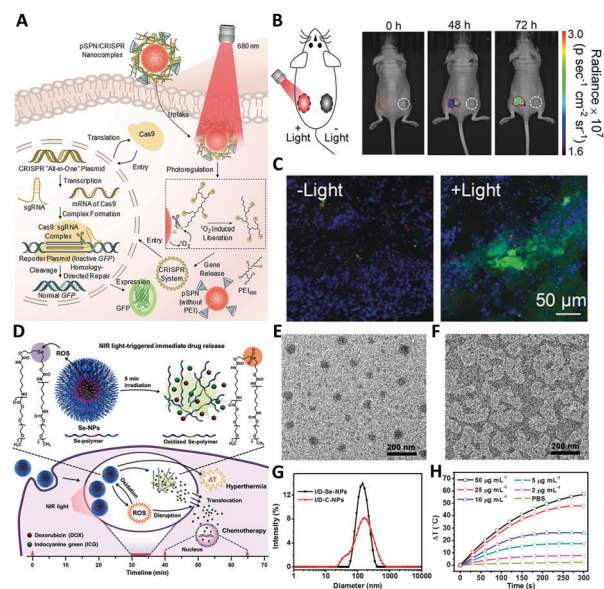


Fig. 4 NIR phototriggered ROS-targeted delivery. (A) NIR phototriggered ROS for on-demand gene editing based on SPN-delivery. (B) Whole-animal fluorescence images at the target location with (left) and without (right) light irradiation (0.3 W cm<sup>-2</sup>, 20 min). (C) CLSM images of slices of mice with or without 680 nm irradiation treatment (72 h) (red: pSPN; green: GFP; blue: cell nuclei). Reproduced with permission from ref. 92. Copyright 2019 Wiley-VCH. (D) Selenium-inserted polymeric nanoparticles with tunable hydrophobicity for delivery and synergistic PTT. (E) Representative TEM image of Se-based nanoparticles. (F) The disassembly of Se-based nanoparticles after irradiation (785 nm, 1.0 W cm<sup>-2</sup>, 3 min). (G) The size distribution of I/D-Se-NPs and I/D-C-NPs. (H) Temperature elevation of the nanomaterials under irradiation after loading different amounts of ICG. Reproduced with permission from ref. 102. Copyright 2017 American Chemical Society.

of DOX for chemotherapy and combined PDT. For the latter, the ROS-adjustable hydrophobicity of thioether, selenoether, telluroether, and histidine derivatives usually contributed to the construction of stimuli-responsive cargo.<sup>102–105</sup> Wang *et al.* have synthesized a selenoether-based polymer for the self-assembly into nanoparticles (Fig. 4D–G).<sup>102</sup> After the encapsulation of ICG and DOX, the nanoassembly was injected in Balb/c mice bearing 4T1 tumors to evaluate its therapeutic effect. The results displayed that NIR-monitoring can assist in suppressing tumor growth and ablate solid tumors by such ON/OFF drug release.

### 3. Near-infrared upconversion activated chemotherapy

NIR light to regulate biological processes often suffers from its low energy and cannot trigger sufficient energy conversion for applications. Upconversion describes a nonlinear optical phenomenon that refers to the generation of high-energy photons (short-wavelength) from two or more low-energy excitation photons (long-wavelength). Over the past decade, a kind of nano-material termed upconversion nanoparticles (UCNPs) that can convert NIR into higher energy (UV/Vis) light has emerged to resolve this issue, providing potential for the realization of photo-controlled biological processes.<sup>106–111</sup> These UCNPs have their excitation wavelengths at 808, 980 and even 1530 nm.<sup>112–114</sup> For precision cancer therapy, UCNPs are not only complemented by ROS-based nanomedicine, but can also be applied to trigger chemical reactions for targeted delivery.

#### 3.1 Upconversion ROS-generating nanoplatforms for cancer treatment

As a novel ingredient of NPDT, UCNPs extended the PDT from the UV/Vis to the NIR window in their own way, which provided an enormous stage for ROS-generation.<sup>115</sup> For example, visual-light triggered cyclometalated iridium(III) complexes with excellent photophysical properties were found as potent PS candidates,<sup>116</sup> and UCNPs endowed the complexes with NIR activation features and realized an NPDT with higher biosafety and <sup>1</sup>O<sub>2</sub> generation efficiency (Fig. 5A).<sup>117</sup> Another work by Chen *et al.* reported an AuNP doped porphyrin MOF@UCNPs (UMOF) for effective cascade driven photodynamic therapy.<sup>50</sup> In the tumor micro-environment, the GOx-like activity of AuNPs triggered glucose depletion and H<sub>2</sub>O<sub>2</sub> generation. Subsequently, the decomposition of the produced H<sub>2</sub>O<sub>2</sub> was performed by the catalysis of the iron porphyrin MOF shell. Upon 980 nm laser irradiation, the UCNPs demonstrated an upconversion luminescence (UCL) emission spectrum with peaks at around 524, 542, and 660 nm which can readily initiate the porphyrin MOF to generate <sup>1</sup>O<sub>2</sub> for PDT against solid tumors (Fig. 5B and C).

#### 3.2 Photochemistry-based delivery nanosystems

Over the past few decades, phototriggered reactions, such as the isomerization of azobenzene and the hydrolytic cleavage of *o*-nitrobenzyl, have been widely explored for on-demand delivery.<sup>118,119</sup> Generally, NIR light hardly triggers chemical

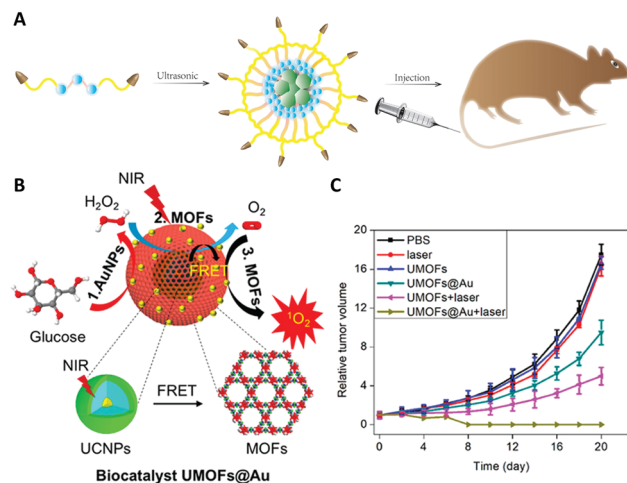


Fig. 5 ROS-generating nanoplatforms based on UCNPs for cancer therapy. (A) Schematic illustration of iridium(III) complex-based micelles for PDT and CDT; reproduced with permission from ref. 117. Copyright 2020 Wiley-VCH. (B) Design of the core-shell UMOFs@Au biocatalyst for combined therapy via cascade catalytic reactions. (C) Relative tumour volumes at different days after different treatments; reproduced with permission from ref. 50. Copyright 2020 American Chemical Society.

reactions due to its low energy. However, the emergence of UCNPs which could provide desirable UV or visible light under NIR irradiation makes it possible, and a myriad of sophisticated reactions have occurred.<sup>120–122</sup>

**3.2.1 Azobenzene-functionalized nanodevices.** Azobenzene and its derivatives have been reported as common light-activated switches with reversible *trans-cis* conformational conversion under different light irradiation, which made it an ideal component for desired light-responsive nanodevices.<sup>123,124</sup> For example, azobenzene groups can be employed in the modification of mesoporous silica-coated UCNPs (UCNP@mSiO<sub>2</sub>) as gatekeepers for NIR light-triggered anticancer strategies,<sup>120</sup> since mesoporous materials with large specific surface areas are regarded as remarkable vehicles for drug delivery. In addition, azobenzene derivatives can be applied to liposomes for NIR-triggered release, which has been detected in MCF-7/ADR cells by Yao *et al.*<sup>125</sup>

Recently, Ju and his colleagues have designed another NIR-light controlled nanodevice based on azobenzene-functionalized DNA strands for on-demand drug release.<sup>126</sup> The nanodevice was fabricated via the assembly of the DNA on UCNPs, and DOX could be loaded in virtue of the high intercalation of DOX and the DNA helix. They discovered that both UV and visible photons from the conversion of NIR contribute to the continuous photoisomerization of azo, leading to subsequent DNA dehybridization and drug release (Fig. 6). After about 30 min irradiation, 86.7% DOX release was obtained in this system. By coating with the HIV-1 TAT cell-penetrating peptide and hyaluronic acid, the nanodevice acquired nuclear-targeted transport capacity and a better inhibition effect on tumor growth was confirmed under 980 nm light irradiation.

**3.2.2 *O*-Nitrobenzyl-based nanomaterials.** A molecule containing *o*-nitrobenzyl moieties, which undergo irreversible ester bond cleavage upon UV irradiation, was developed as an important



Fig. 6 Azobenzene-functionalized nanodevices for delivery. (A) Schematic illustration of the design and working mechanism of Azo/DOX/DNA assembly on UCNPs. (B) HA and TAT-modified Azo/DOX/DNA assembly for improved target transfection. (C) Processes of endocytosis mediated by HA, nuclear targeting enhanced by TAT, and DOX release triggered by NIR light. (D) The DOX release profiles of UCNPs-LAAzoBCAzo/DOX and UCNPs-LABC/DOX under NIR light exposure. (E) Tumour growth curves of mice bearing HepG2-derived tumors subjected to various treatments. Reproduced with permission from ref. 126. Copyright 2019 Wiley-VCH.

building block of light-controlled nanodevices for a myriad of bio-applications ranging from cell manipulation to targeted therapy.<sup>107,127–130</sup> In combination with UCNPs, these nanodevices have been extensively explored for the on-demand release of drugs including small molecules and biomacromolecules. For example, our group developed a NIR light-responsive cargo for the delivery of CRISPR-Cas9 based on 4-(hydroxymethyl)-3-nitrobenzoic acid (ONA)-functional UCNPs (Fig. 7A).<sup>131</sup> Under NIR irradiation, the UCNPs emit UV light leading to the cleavage of photosensitive molecules for the release of CRISPR-Cas9. The results showed that, when engineering the single guide RNA to target *polo-like kinase-1* (*PLK1*, a tumor gene), the cell apoptosis could be successfully initiated both *in vitro* and *in vivo* by NIR light-triggered gene editing.

Compared with covalently linking to photosensitive molecules, the drug was encapsulated into a photo-degradable network without chemical modification, which seems to be a more convenient method. Zhou *et al.* synthesized two polymers: an amphiphilic polymer (iPHT) modified with iRGD at both ends and another one (HTMP) based on PEG containing *o*-nitrobenzyl (Nbz) linkers and poly( $\beta$ -aminoesters) (a pH-sensitive hydrophobic segment);<sup>132</sup> then UCNPs and the drug (DOX in this study) were mixed with the aforementioned polymers to prepare a hybrid nanocomposite *via* an ultrasonic-assisted solvent-substitution method. In these systems, UCNPs could convert NIR to UV light to cleave the Nbz linkers for the dissociation of the nanocomposite in tumors with acidic environments under deep tissue. In addition, the authors found that the NIR-induced photochemical reaction caused the dePEGylation of nanoparticles but improved the cellular uptake, which effectively assisted the inhibition of tumor growth (Fig. 7B–E).

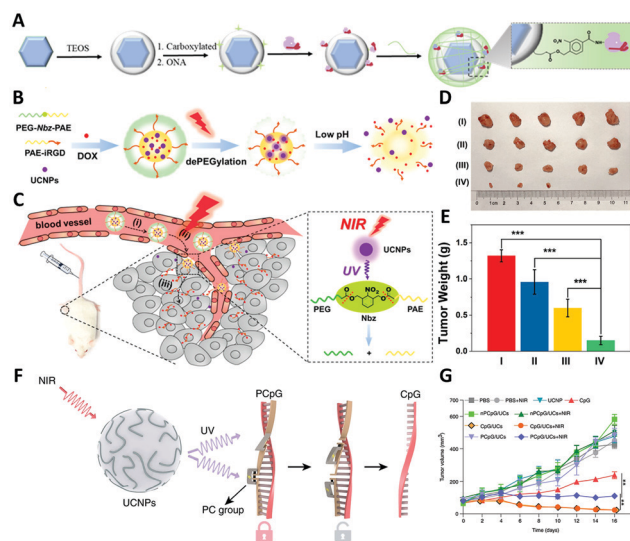


Fig. 7 *O*-Nitrobenzyl-based drug delivery. (A) The design of a light-controlled gene editing nanoplatform based on nitrobenzyl chemistry; reproduced with permission from ref. 131. Copyright 2019 American Association for the Advancement of Science. (B) Illustration of light/pH responsive delivery. (C) NIR-guided nanosystem to overcome the physiological barriers (i) blood circulation; (ii) extravasation; (iii) tumour penetration. (D) Photographs and (E) average weight of the resulting tumours treated using (I) PBS + NIR light, (II) free DOX + NIR light, (III) iPUDN, and (IV) iPUDN + NIR light (mean  $\pm$  SD,  $n = 5$ ; \*\*\*  $P < 0.001$ ); reproduced with permission from ref. 132. Copyright 2019 American Chemical Society. (F) The conduction of programming of a photoactivatable immunodevice by combining UCNPs with the UV light-responsive PCpG. (G) Tumor growth curves treated using different samples with or without NIR irradiation. Reproduced with permission from ref. 133. Copyright 2019 Springer-Nature.

Photocleavable (PC) bonds (*o*-nitrobenzyl moieties) were also introduced in ssDNA to design a NIR light-activated immunodevice for spatiotemporal manipulation of the immune reaction *in vivo* with less systemic toxicity.<sup>133</sup> This methodology employed the hybridization of CpG oligonucleotides (CpG, an immunotherapeutic agent) and its complementary ssDNA with PC groups (PcDNA) to prevent the activation of toll-like receptor 9 (TLR9) by CpG in immune cells (Fig. 7F and G). UCNPs in this approach were applied as nanovehicles for CpG delivery to enhance the transfection efficiency of ODNs and their accumulation in tumor tissue. To trigger immunoactivation, NIR light was turned on at the target location to yield local UV light by UCNPs for breaking the PC group of PcDNA and liberating the CpG. The controlled systemic administration of CpG allows effective immune regulation at the target location without the initiation of immunity elsewhere in the body and thus could maintain the cancer-combating property with less systemic toxicity.

**3.2.3 Light-activated prodrugs.** Typically, a prodrug serves as a molecule with satisfactory biocompatibility that, after administration, can be transformed into a pharmacologically active drug by endogenous or exogenous stimuli.<sup>134–136</sup> Plenty of research has confirmed the on-demand anticancer effect of prodrug strategies with minimal systemic toxicity.<sup>135</sup> When combined with UCNPs, prodrugs are endowed with tissue-penetrable activity and act as chemotherapeutic reagents under NIR light, such as platinum(II)



**Fig. 8** Light-activated prodrug. (A) Intracellular localized SO<sub>2</sub> generation upon NIR light irradiation for cancer therapy. (B) Relative tumor volumes, (C) survival curves, and (D) body weights under different treatments. Reproduced with permission from ref. 146. Copyright 2019 American Chemical Society.

compounds and nitric oxide (NO).<sup>137–143</sup> Also, the Pt(IV) prodrug can be designed for NIR photocleaved chemotherapy based on UCNP. The UV light from UCNP and the tumor microenvironment contributed to the targeted generation of the Pt(II) drug to damage DNA for antitumor therapy.<sup>144,145</sup> Recently, a NIR-controlled supply platform of SO<sub>2</sub> was developed for augmenting the antitumor therapies based on rattle-structured UCNP@porous silica nanoparticles.<sup>146</sup> In this case, 1-(2,5-dimethylthien-1,1-dioxide-3-yl)-2-(2,5-dimethylthien-3-yl)-hexafluorocyclopentene (DM) served as a prodrug, which can rapidly turn into an open-ring isomer under irradiation at 365 nm to supply SO<sub>2</sub> (Fig. 8). The authors have evaluated the biosafety and *in vivo* antitumor efficacy of such nanogenerators, and a satisfactory phenomenon was observed in which a higher intracellular ROS level from the existence of SO<sub>2</sub> resulted in damage to the DNA nucleus and subsequently tumor inhibition at the target location without engendering adverse effects.

**3.2.4 Other light-responsive nanomaterials.** The mechanisms of photosensitivity can be roughly divided into photocross-linking/-decross-linking, photocleavage, and photoisomerization. For the photocross-linking/-decross-linking strategy, coumarin and its derivatives were confirmed to cross-link with each other under UV irradiation, which can be employed for drug delivery.<sup>147</sup> As for photocleavage, ruthenium (Ru) complexes have been reported as gatekeepers on the surface of UCNP@mSiO<sub>2</sub>, and the feasibility of the system has been proved in HeLa cells by incubation with DOX-UCNP@mSiO<sub>2</sub>-Ru.<sup>148</sup> As for photoisomerization, spiropyran and its derivatives are typical examples to be used in a controllable strategy.<sup>149</sup> They can become hydrophilic from hydrophobic under high-energy light irradiation owing to the formation of a ring-opening structure, which was grafted onto mesoporous silica-coated UCNP (UCNP@mSiO<sub>2</sub>) to control drug access.<sup>150</sup> Specifically, in the hydrophobic spiropyran layer, hydrophobic drugs could be sealed in the pores of silica, whereas the hydrophilic spiropyran layer caused by local UV light from UCNP upon NIR irradiation would lead to the release of the drug for therapy. In another case, 2-diazo-1,2-naphthoquinones (DNQs) were found to act as hydrophobic-to-hydrophilic switches as well.<sup>151</sup> The authors proposed NIR-controlled drug delivery

using immobilized hydrophobic DNQs on UCNP@mSiO<sub>2</sub> as guest molecules. Before the NIR laser was turned on, β-cyclodextrin (β-CD) host molecules capped the DNQs to prevent the leakage of drugs *via* the hydrophobic affinity of DNQs and the hydrophobic cavities in β-CD. Thus, subsequent 980 nm light illumination could dismiss the β-CD and activate the ON state of drug release in virtue of the generation of the hydrophilic guest 3-indenecarboxylic acid (ICA) from DNQs.

## 4. Near-infrared photothermal cancer nanotherapy

Temperature-sensitive nanosystems, which underlie the clinical adaptation for non-invasive treatment, are driving researchers to unearth their full potential for biomedical advances.<sup>152,153</sup> However, direct precise manipulation of temperature *in vivo*, especially in deep tissues, seems to be hard to achieve. Thanks to the boom of nanotechnology, photothermal conversion of nanomaterials endows these systems with spatiotemporal selectivity for tumor treatment.<sup>153</sup>

### 4.1 Photothermal therapy (PTT)

Thermal energy not only contributes to our whole lives and to industry, but can also be deployed to clinically combat cancer, for example, hyperthermia.<sup>154</sup> Typically, the remedy requires local temperature above a threshold value for a certain time before tumor ablation, for example, 50 °C lasting for 4–6 min.<sup>155,156</sup> Since some materials that can effectively absorb photons to generate heat energy were discovered, light-mediated hyperthermia (termed PTT) has gradually become popular in hyperthermia due to its noninvasive mode and high spatiotemporal precision.<sup>157,158</sup> The photothermal effect describes a phenomenon wherein materials absorb photons (commonly in the NIR window) and transform it into localized heat. The resulting heat can be employed for precise hyperthermia through rational design, which is also named photothermal therapy (PTT), a spatiotemporally controllable remedy.

**4.1.1 The commonly adopted PTAs.** After the mechanism of nanomaterial-based PTT became clearer, more and more research studies on the development of sophisticated nanomaterials as photothermal agents (PTAs) to destroy solid tumors were reported.<sup>159–161</sup> In this section, we focus on recently developed nanoagents which were used for NIR light-induced PTT.

**Inorganic PTAs.** Au nanomaterials were widely used as inorganic PTAs with the surface plasmon resonance (SPR) effect, and many studies have confirmed their practical value for PTT.<sup>162,163</sup> Other inorganic nanomaterials including single-walled carbon nanotubes, carbon dots, MoO<sub>3-x</sub> nanoparticles, and magnetic nanoparticles with broad absorption ranging from UV to NIR can also convert NIR light directly into heat energy for photothermal ablation of mouse tumor xenografts.<sup>164–172</sup> In addition, the recent emergence of two-dimensional (2D) nanomaterials provides an original type of PTAs for the maximization of the PTT effect.<sup>173–175</sup> For example, the ultrathin MXenes from layered ternary carbides of MAX phases, which served as multifunctional 2D materials



prepared by A-element etching methods, were explored for available PTT by Shi's group.<sup>176,177</sup> Here, M in MAX represents a transition-metal carbide (*i.e.* Ti, V, Zr), A stands for an element mostly in groups 13 and 14, and X represents carbon or nitrogen. In addition, 2D black phosphorus (BP) demonstrated extraordinary biocompatibility with both photothermal and photodynamic characteristics and is among the most promising candidates of photo-activatable therapeutic agents as well.<sup>178</sup>

**Organic PTAs.** Over the past decade, polydopamine (PDA) has undergone active research as both nanoparticles and surface coating (film) materials owing to its impressive properties, such as its remarkable affinity to a large number of metals/metal ions, antioxidant activity, and so on.<sup>179,180</sup> Inspired by these properties, Poinard *et al.* utilized the near-infrared photothermal property of PDA nanoparticles to kill cancer cells, and after loading Ce6 an enhanced antitumor effect was observed on account of the combined PDT + PTT.<sup>181</sup> Another organic optical nanoagent, SPNs, without metal-ion-induced toxicity demonstrated size-independent optical properties different from most semiconductor inorganic nanoparticles.<sup>83</sup> An example of the use of SPNs for PTT was demonstrated by Yang *et al.*<sup>182</sup> In that case, an SPN-based system called L1057 NPs was reported for PTT under NIR irradiation (720 mW cm<sup>-2</sup>), and interestingly fluorescence imaging can also be achieved with the assistance of a low (25 mW cm<sup>-2</sup>) laser fluence. Additionally, there exists a great number of other organic PTAs to suppress tumor growth *in vivo*, including hair nanoparticles (HNPs) from the micrometer-sized melanosomes of our human hair,<sup>183</sup> and covalent organic frameworks (COFs) from synthetic small molecules.<sup>184</sup>

In addition to the aforementioned examples, other interesting in/organic nanomaterials that can serve as PTAs are also worth studying.<sup>185–188</sup> Some commonly adopted PTAs and their corresponding performance are listed in Table 1.

**4.1.2 The potential strategies for near-infrared photothermal-assisted therapy.** Generally, a single treatment, for example, PTT alone, hardly realizes considerable outcomes, and thus the “1 + 1 > 2” combined therapy strategies have become a vigorous trend. Very recent treatment combinations with PTT include photodynamic therapy, chemotherapy, and immunotherapy, and a lot of papers reported the outstanding effect *via* such synergized modality.<sup>87,189–192</sup> However, reviews on the combination strategies can be readily found, and for ease of elaboration, we are going to be more involved in discussing the future of PTT alone in the following.

**Mild temperature.** Typically, the currently available PTT requires a relatively high temperature over 50 °C, which damages normal tissues as well. Therefore, how to achieve effective cancer therapy strategies using mild temperature conditions becomes an inevitable challenge for PTT. As previously reported, the hyperthermia effect at 42–47 °C is closely associated with heat shock protein (HSP), which demonstrates molecular chaperone functions, and can immediately repair the intracellular protein damage from heat.<sup>193,194</sup> Hence, it is expected to address the thermoresistance of cells *via* HSP inhibition. To date, several HSP inhibitors have been successfully applied for low-temperature photothermal therapy.<sup>155,191,195–200</sup> For example, Ding *et al.* have developed a strategy to improve the mild-temperature PTT efficiency by using small interfering ribonucleic acid (siRNA) targeted Hsp70 as a crosslinker.<sup>197</sup> In this system,

Table 1 Summary of commonly adopted PTAs (N.A.: not applicable)

Classification	Typical nanomaterials	Irradiation wavelength (nm)	Irradiation power density (W cm <sup>-2</sup> )	PCE (%)	Biological model	Ref.
Inorganic nanomaterials	Au-Based nanomaterials (spiky Au NPs)	980	0.8	78.8	HepG2 cells	208
	Fe <sub>3</sub> O <sub>4</sub>	808	3	~37	A549 cells	171
	WO <sub>3-x</sub>	808	0.5	N.A.	4T1 cells	186
	(NH <sub>4</sub> ) <sub>x</sub> WO <sub>3</sub> nanocube	1064	1.4	39.4	4T1 cells	204
	MoO <sub>x</sub>	808	1.0	41.24	HeLa cells	165
		808	1.0	36.72	4T1 cells	78
	CuS	808	0.987	N.A.	4T1/A549 cells	168
	WS <sub>2</sub>	808	1.0	N.A.	HeLa cells	170
	MoS <sub>2</sub>	808	0.4	N.A.	MCF-7 cells	30
	FePS <sub>3</sub>	1064	1.0	43.3	HeLa cells	206
	Black phosphorus	808	0.5	N.A.	MCF-7 cells	174
	Graphene-based nanomaterials	808	2.0	N.A.	4T1 cells	175
	Mo <sub>2</sub> C-Derived polyoxometalate	1060	1.0	47.8	HeLa cells	205
	MXenes	808	1.5	30.6	4T1 cells	176
		808	1.5	44.7	4T1 cells	177
	Organic nanomaterials	COF (Py-BPy+ • -COF/PEG)	808	1.0	63.8	A549 cells
		1064	1.0	55.2		
Hair particles		808	1.0	N.A.	4T1 cells	183
tfm-BDP		808	0.3	88.3	HeLa, MCF-7, and 4T1 cells	207
Inorganic/organic nanohybrids	SPNs (L1057 NPs)	980	0.72	38	4T1 cells	182
	PDA	808	2.0	~40	HeLa cells	180
	MOF (Zr-PDI* <sup>-</sup> )	808	0.7	52.3	N.A.	185
	PDA coated Au plasmonic blackbodies	808	0.33	88.6	4T1 cells	209
		1064	1.0	80.8		
	MoS <sub>2</sub> quantum dot@PDA nanohybrids	808	1.5	31.6	4T1 cells	188
Fe <sup>3+</sup> -Induced polypyrrole nanoparticles	808	1.5	43.6	4T1 cells	187	

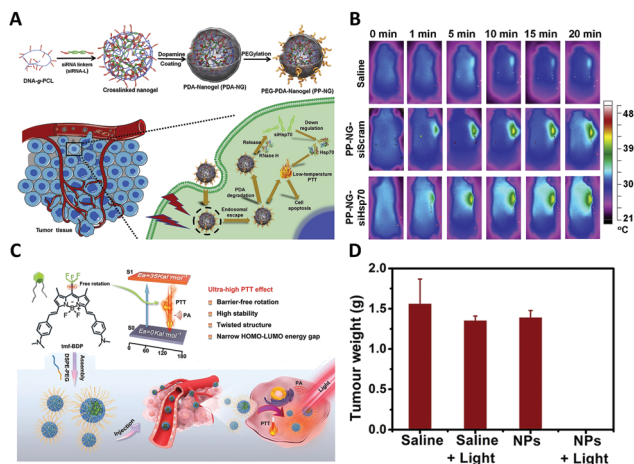


**Fig. 9** Strategies for PTT enhancement. (A) Scheme of the polydopamine-coated nanogel bearing siHSP70 for low-temperature photothermal therapy. (B) Infrared thermal images of mice after different treatments under NIR laser irradiation; reproduced with permission from ref. 197. Copyright 2020 Elsevier Inc. (C) A PTA with a high PCE for phototherapy: (a) molecular structure of tfm-BDP; (b) barrier-free rotation of CF<sub>3</sub> for enhanced heat production (the X axis displays the rotation angle of CF<sub>3</sub>); and (c) the tfm-BDP nanoparticle guided PA imaging for PTT. (D) The tumor weights in each group. Reproduced with permission from ref. 207. Copyright 2020 Wiley-VCH.

siRNA loaded in a polydopamine-coated nucleic acid nanogel triggered the associated intracellular gene silencing and the subsequent inhibition of Hsp70 expression, which realizes PTT at mild-temperature with remarkable cancer destruction efficacy (Fig. 9A and B). Furthermore, other HSP inhibitors including 17-allylamino-17-demethoxygeldanamycin (17-AAG) and gambogic acid (GA) have been confirmed to be effective to assist mild-temperature PTT.<sup>195,201</sup> Additionally, researchers discovered that HSP is intrinsically subjected to adenosine triphosphate (ATP), and thus glucose consumption by GOx, which limited the ATP supply, also enhanced the mild-temperature PTT *via* downregulation of the expression of HSP.<sup>198</sup>

Recently, an interesting precisely temperature-controlled photothermal therapy was designed using reversible thermochromic nanoparticles, which were prepared by simple self-assembly of water-soluble poly(ethylene glycol) (PEG), a leuco dye, (2'-phenylamino)-6'-(diethylamino)fluoran, TFG), and a developer ( $\beta$ -naphthol).<sup>200</sup> In this thermochromic system, a temperature below 45 °C endowed such nanoparticles with dark-green color and absorption at 620 nm, yet a complete depigmentation and no photon absorption can be observed when the temperature was increased up to 45 °C, which provided a brilliant way to maintain the temperature at a predefined transition point (45 °C) for safer cancer therapy. Specifically, TFG can transform NIR light into heat and increase the surrounding temperature at the target site. When the temperature reached 45 °C, the colored nanoparticles will display a colorless state for preventing the absorption of NIR light and maintaining the temperature. *In vivo* experiments have confirmed the precisely controlled PTT without overheating the surrounding tissue.

**Down wavelength.** The less energy attenuation of a longer wavelength allows deeper tissue penetration, for instance, NIR-II

light obtains an increased tissue penetration of 30–50 cm, while NIR-I light corresponds to 10 mm,  $\lambda = 705$  nm reaches  $7.5 \pm 0.5$  mm, and  $\lambda = 408$  nm obtains  $1.0 \pm 0.02$  mm.<sup>32,202</sup> Considering the different components of animal tissues, the inhomogeneity of refractive indices is inevitable, which lead to different exponents for wavelength dependence, for example,  $\mu = 1.72 (\lambda/\mu\text{m})^{-0.65}$  for cranial bone,  $4.72 (\lambda/\mu\text{m})^{-2.07}$  for brain tissue,  $0.61 (\lambda/\mu\text{m})^{-1.62}$  for mucous tissue, and  $0.56 (\lambda/\mu\text{m})^{-1.045}$  for muscle.<sup>39</sup> Therefore, it is of great significance and high desirability to explore PTAs for cancer therapy in a farther window (*i.e.*, NIR-II at 1000–1350 nm).<sup>202</sup> A myriad of SPNs with remarkable optical properties have been found to respond to light of various wavelengths including UV, NIR-I, and even NIR-II, which were confirmed as efficient PTAs for photoacoustic (PA) imaging-guided photothermal therapy.<sup>203</sup> Jiang *et al.* prepared an SPN with two intrinsic absorbance peaks at 808 and 1064 nm, and the SPN shared similar photothermal conversion efficiencies at different wavelengths (44.9% for 808 nm and 43.4% for 1064 nm), which offer an opportunity for comparison of different therapeutic efficacies in NIR-II and NIR-I windows. The results verified that the SPN showed superior deep-tissue heating and an enhanced PTT effect at 1064 nm over that at 808 nm. In other studies, the rational design of Au-based nanoparticles, such as the hybridization of Au NPs with CuS or Ag, was found to make the absorption experience redshift to the NIR-II window, and achieved a better anticancer effect. Moreover, a kind of inorganic nanomaterials with a broad absorption range covering 1000–1350 nm can act as NIR-II PTAs as well, including 2D FePS<sub>3</sub>,<sup>204</sup> Nb<sub>2</sub>C nanosheets,<sup>205</sup> and (NH<sub>4</sub>)<sub>x</sub>WO<sub>3</sub> nanocubes,<sup>206</sup> and the results showed that these PTAs displayed excellent photothermal efficiencies in both NIR-I and NIR-II windows, and efficient photothermal ablation of tumors.

**High photothermal conversion efficiency.** The photothermal conversion efficiency (PCE) of PTA constituted another inevitable key issue that remains to be addressed in PTT.<sup>207</sup> Generally, the PCEs of PTAs were nearly impossible to reach 100% due to their composition and structural details, and most of the current PTAs were developed with PCEs below 50%. Recently, Bi *et al.* synthesized a kind of spiky Au NPs with 6 spikes on a small core, which demonstrated an ultra-high PCE of 78.8% under 980 nm irradiation.<sup>208</sup> In addition, a PDA coated Au plasmonic blackbody (AuPB) with PCEs of 88.6% at 808 nm and 80.8% at 1064 nm was reported. Furthermore, organic PTAs can also achieve high PCEs.<sup>209</sup> For example, in 2019, Liu *et al.* developed a terrylene-dimide chromophore-based PTA which demonstrated a high PCE of about 64.7%, and a remarkable PTT effect was successfully achieved both *in vitro* and *in vivo*.<sup>210</sup> A year later, Peng's group improved the PCE to 88.3% based on novel organic PTAs, which was modified with a CF<sub>3</sub> moiety on the meso-position of the BODIPY scaffold (tfm-BDP)<sup>207</sup> (Fig. 9C and D). The authors noticed that the CF<sub>3</sub> performed with a free energy barrier to rotation in both excited and ground states, leading to ultra-efficient non-radiative decay for the highest PCE. Surprisingly, the tfm-BDP can be formulated into polymeric nanoparticles *via*  $\pi$ - $\pi$  stacking and remains barrier-free for the CF<sub>3</sub> moiety. By means of 808 nm laser irradiation ( $0.3 \text{ W cm}^{-2}$ ), complete tumor ablation

can be readily accomplished *in vivo*, where the polymeric nanoparticles accumulated through intravenous injection.

## 4.2 Photothermal drug release

Light-generated heat not only directly results in hyperthermia for cancer treatment, but can also be employed for controlled release as a switch. As low-grade energy, heat demonstrated relatively low effective utilization and only acted on some weak chemical bonds. Hydrogen bonds constitute one of those, which is associated with the environmental temperature, and thus DNA-based nanodevices and phase-change materials (PCMs) with the hydrogen-bond established structure are endowed with thermosensitive features. In this section, we summarized the currently available common photothermal induced delivery systems which relied on nanomaterials for cancer treatment.

### 4.2.1 Complementary base pairing controlled delivery.

Complementary base pairing is founded on the generation of a specific hydrogen bond between purines aligned with pyrimidines, which is strongly related to temperature.<sup>211,212</sup> Some small molecule drugs, such as doxorubicin (DOX), can intercalate into DNA/RNA double-stranded regions and form a physical conjugate *via* noncovalent intercalation, which inspired researchers to develop base pairing-based nanoplatforams for drug delivery and eradication of cancers and solid tumors.<sup>213</sup> In 2016, a facile core-satellite drug (Dox was used in this work) nanocarrier was designed by DNA hybridization.<sup>214</sup> When the laser was turned on, the Dox-loaded DNA duplex would dehybridize due to the high local heat and thus release the drug (Fig. 10A and B). Similarly, He *et al.* have synthesized another DNA-functionalized gold nanorod (AuNR) which was capped with TiO<sub>2</sub> at both ends for DOX-photothermal delivery and PTT.<sup>215</sup> With the assistance of a photosensitizer (ICG was used here), such TiO<sub>2</sub>-capped AuNRs can also be applied for <sup>1</sup>O<sub>2</sub> production to augment the anticancer effect. Alternatively, DNA hybrids are great gate-keepers for mesoporous nanomaterials, and such mesoporous silica-coated Cu<sub>1.8</sub>S nanoparticles were designed as 980 nm-laser triggered nanovehicles.<sup>216</sup> In this study, curcumin (a dietary polyphenol constituent for the inhibition of tumor cell growth) would be released from the mesopores of silica and the Dox-DNA conjugate was dissociated upon NIR irradiation.

In addition to small-molecule drugs, NIR-controlled nanovectors for DNA/RNA delivery were successfully achieved through functional photothermal nanomaterials. To our knowledge, there are some oligonucleotides which could regulate the gene expression and affect cell activity or proliferation, such as CpG, and hence targeted nucleic acid delivery exhibits great significance for convenient and safe gene interference-based therapeutics. In 2019, Liang's group developed DNA-mediated self-assembled Au-DNA nanosunflowers with NIR-controllable transformation for gene silencing.<sup>217</sup> Specifically, thiol-oligonucleotides (POY2T, which can be used to down-regulate *c-myc* expression<sup>218</sup>) modified 2-nm Au NPs and CA (a single-stranded sequence which complementarily hybridized with a part of POY2T) self-assembled into large-sized sunflower-like structures which displayed high photothermal conversion ability (Fig. 10C and D). After NIR illumination, the nanosunflowers would disassemble due to the breakage of a specific hydrogen bond between CA and POY2T,

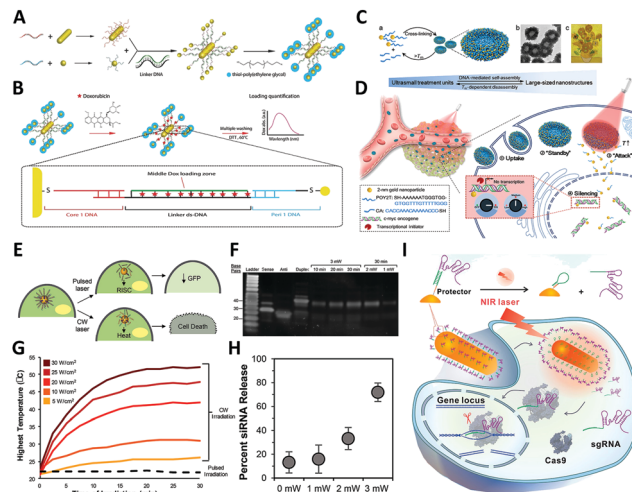


**Fig. 10** Complementary base pairing-based controlled delivery. (A) Design of Au core-satellite superstructures *via* DNA assembly. (B) The DNA linker strands for Dox loading and the resulting absorption measurements; reproduced with permission from ref. 214. Copyright 2016 Wiley-VCH. (C) (a) Assembly and disassembly of the ultrasmall nanoparticles (2 nm Au-POY2T NPs) based on Tm. (b) TEM image of the sunflower-like nanostructures. (c) The masterpiece from Vincent van Gogh (1889). (D) The light controlled gene silencing by the photothermal effect: (1) cellular uptake of large-sized nanosunflowers; (2) the superparticles on standby in cells; (3) NIR phototriggered dissociation of nanosunflowers; (4) realizing gene silencing; reproduced with permission from ref. 217. Copyright 2019 American Association for the Advancement of Science. (E) The mechanism of gene regulation with siRNA-NS conjugates. (F) Gel electrophoresis for evaluating the siRNA releasing effect at different powers and times. (G) Bulk solution temperature measurement under 808 nm irradiation (solid lines: CW laser; black line: pulsed laser). (H) Time dependence of pulsed light (3 mW)-induced siRNA release; reproduced with permission from ref. 221. Copyright 2018 American Chemical Society. (I) Hybridization of sgRNA and a protector DNA on a gold nanorod for light controlled gene editing based CRISPR system; reproduced with permission from ref. 222. Copyright 2020 American Chemical Society.

and subsequently the smaller 2 nm Au-POY2T NPs attacked the cell nucleus, thus achieving gene regulation. Further *in vivo* experiments demonstrated that nanosunflowers upon light irradiation could significantly enhance tumor growth inhibition.

MicroRNAs (miRNAs) represent noncoding single-stranded RNAs that are associated with several biological processes, such as cell proliferation and survival,<sup>219</sup> and hence on-demand delivery of miRNAs displays a broad application range. Recently, a NIR-activated miRNA releasing nanosystem was developed by the hybridization of derived miR-dsDNA and AuNR, and was proved valid in a wound-healing experiment.<sup>220</sup> In another work by Emily S. Day and co-workers, small interfering RNA (siRNA)-coated silica core/gold shell nanocomposites were achieved for NIR light-controlled gene regulation.<sup>221</sup> They found that a pulsed laser can release duplex siRNA through a temperature-independent process for the recognition of RNA induced silencing complex (RISC) and reduce the level of target gene (GFP) expression, without affecting the temperature of the bulk solution, whereas CW irradiation resulted in a dramatically increased temperature of the bulk solution, both single-stranded siRNA and duplex release, and nonspecific cell death rather than

desired gene silencing (Fig. 10E-H). Moreover, these complementary base pairing rules were applied to control the RNA-guided CRISPR/Cas9 system.<sup>222</sup> As shown in Fig. 10I, a protector DNA that can hybridize to sgRNA was caged on AuNRs. Owing to the efficient photothermal conversion of AuNRs, the sgRNA could release from the protector and initiate gene editing. The cell experimental results confirmed the efficient delivery of sgRNA and the NIR-controlled release of sgRNA for target gene (EGFP and PLK1) knock.

**4.2.2 Phase-change controlled delivery.** With the potential to serve as thermoresponsive gating materials, wax materials are referred to as fatty acid analog phase-change materials (PCMs) which enveloped drugs in the hydrophobic region for photothermal controlled release.<sup>223,224</sup> Xia's group also prepared a nano-eutectic mixture with a melting point at 39 °C by using naturally occurring fatty acids (lauric acid and stearic acid in this report) with remarkable biocompatibility and biodegradability.<sup>225</sup> After encapsulating DOX and IR780 iodide (IR780, a NIR-absorbing dye), the nanoparticles were decorated with lecithin and DSPE-PEG5000 and exhibited NIR-light responsivity for drug delivery. In another similar study, Dong's group has developed a PCM with a melting point at about 45 °C by mixing oleic acid (OA) and 1-hexadecanol (Hex).<sup>226</sup> They packed sub-10 nm  $\text{ZnGa}_{1.996}\text{O}_4\text{:Cr}_{0.004}$  (ZGC, a kind of persistent luminescence materials) nanoparticles and IR780 in the phase-change nanoparticles, which exhibited good biocompatibility under NIR irradiation, as the PDT effects were inhibited by the isolation between IR780 and the outside environment (Fig. 11A). Nevertheless, the results showed that the wax-seal environment would strengthen the photothermal performance of ZGC and IR780. Thus, NIR irradiation readily caused melting of the PCM shell, leading to the generation of ROS as pre-exciting ZGC persistently transfers energy to IR780. Besides, ZGC sealed in PCM can contribute to strong photoluminescence (PL) emission for afterglow imaging and guided target tumor ablation *in vivo*.

Poly(*N*-isopropylacrylamide) (PNIPAM) and its derivatives or copolymers are the most popular forms of thermoresponsive polymers, holding great potential in biomedical applications.<sup>227–229</sup> Generally speaking, polymers demonstrate hydrophilicity with higher solubility at temperatures below their lower critical solution temperature (LCST, also called the cloud point), while it is contrary when the temperature is above the LCST.<sup>230</sup> Based on that, hollow  $\text{mSiO}_2$ , grafted on a PNIPAM derivative with an LCST at 45 °C, loaded indocyanine green (ICG, a photothermal conversion agent) and DOX were used for NIR light-triggered chemotherapy. With NIR irradiation, polymers become more hydrophilic to uncover the mesoporous channel for drug release.<sup>231</sup> The experiments witnessed the higher anticancer efficiency of the delivery system.

Lipids with a hydrophilic polar headgroup and a hydrophobic tail(s) can self-assemble into nanostructures, such as vesicles, in aqueous solution. They were flourishing in drug delivery and plasma membrane models. Many studies suggested that the nanostructures were affected by the environmental temperature. For example, a lipid composed of 1,2-dipalmitoyl-*sn*-glycero-3-phosphocholine (DPPC) and 1,2-distearoyl-*sn*-glycero-3-phosphoethanolamine-poly(ethylene glycol) 2000 (DSPE-PEG2000) demonstrated a

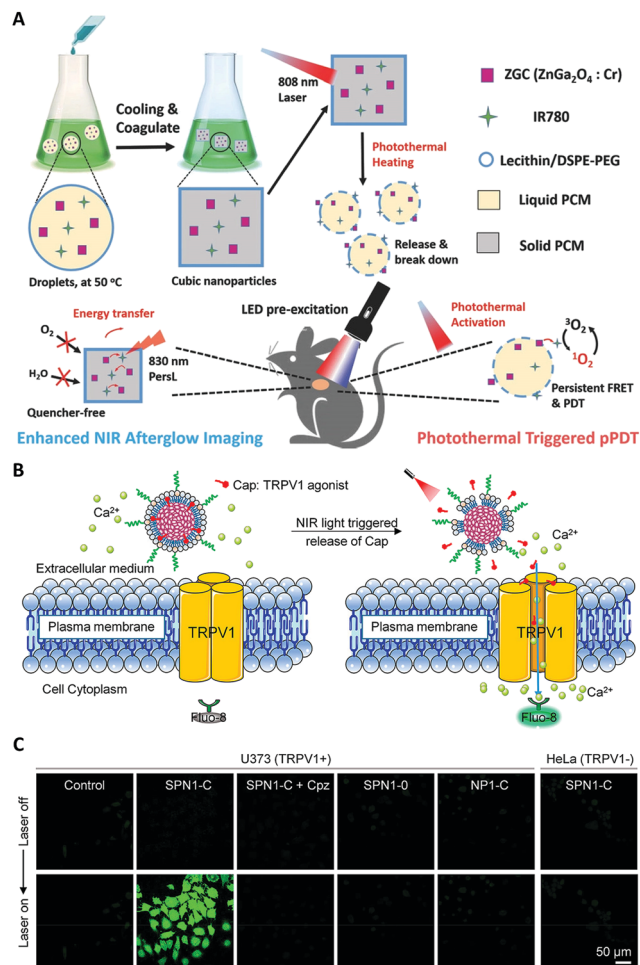


Fig. 11 Phase-change materials for on-demand delivery. (A) Illustration of the PCM loading IR-ZGC for enhanced imaging and PDT; reproduced with permission from ref. 226. Copyright 2018 Wiley-VCH. (B) Schematic diagram of the activation of TRPV-1  $\text{Ca}^{2+}$  channels triggered by NIR-light and the real-time surveillance of intracellular  $\text{Ca}^{2+}$  concentration by Fluo-8 with turn-on fluorescence after binding with  $\text{Ca}^{2+}$ . (C) Fluorescence images of U373 and HeLa cells under treatment with different SPNs (SPN1-C, SPN1-0 and NP1-C) with or without 808 nm ( $\sim 0.4 \text{ W cm}^{-2}$ ) laser irradiation for 35 s; reproduced with permission from ref. 232. Copyright 2018 American Chemical Society.

phase-transition temperature of 41 °C, which offered a chance for NIR-photothermally controlled drug delivery. Recently, a NIR controlled photothermal nanoagonist, which was based on such a lipid, was developed for specific cancer treatment.<sup>232</sup> In the system, the authors loaded 8-methyl-*N*-vanillyl-6-nonenamide (capsaicin, an agonist for transient receptor potential cation channel subfamily V member 1 (TRPV1)) on SPNs and sealed the resulting nano-composite into lipids. Once the NIR-light was turned on, the generation of heat converted by SPNs could damage the nanostructures and release the agonist to activate  $\text{Ca}^{2+}$  ion-channels (Fig. 11B and C). As the over-activation of TRPV1 channels could initiate cell death by overinflux of  $\text{Ca}^{2+}$  ions, the apoptosis of TRPV1-positive tumors would occur under the control of NIR light irradiation.

**4.2.3 NIR-biochemistry triggered drug delivery.** Temperature serves as an issue parameter for chemical processes. Thus PTAs

can be employed to control chemical reactions for on-demand delivery via photothermal conversion effect. For example, some reports claimed that Au-S bonds would break under NIR irradiation owing to the generation of heat from Au nanoparticles, and the system was confirmed to be available for biomacromolecule delivery.<sup>233</sup> Boronic ester linkages also undergo a reversible reaction and can be controlled by heat monitoring. Very recently, Kuang's group modified Au nanoparticles with 4-(4-(aminomethyl)-1,3,2-dioxaborolan-2-yl)benzenethiol (AMDBT) and then connected them to the carboxy-modified DNA. The resulting nanoparticles and Granzyme B and peptide CFDEVK-Cy5.5-comodified UCNPs can self-assemble into upconversion-nanoparticle (UCNP)-centered Au nanoparticle tetrahedrons (UAuTe) by DNA hybridization (Fig. 12A and B).<sup>234</sup> *In vivo*, NIR light triggered the breakage of boronic ester linkages and led to the disassembly of the UAuTe, thereby releasing the Granzyme B on the UCNPs to assist the clearance of senescent cells. Due to the breakage of the peptide CFDEVK by caspase 3 (a downstream protease of apoptosis), which damaged the fluorescence resonance energy transfer (FRET) between the UCNPs and Cy5.5, the UAuTe can be employed as an indicator to track the apoptosis process.

NIR-chemistry can also be used to activate prodrugs for cancer treatment. To our knowledge, the azo initiator 2,2'-azobis(2-(2-imidazolin-2-yl)propane)dihydrochloride (AIPH) and some gas donors (*i.e.* *S*-nitrosothiols, ammonium bicarbonate) constitute the common heat-sensitive prodrugs.<sup>139,143,235–237</sup> In a study by Ding *et al.*, they synthesized a kind of *S*-nitroso (SNO, a heat-sensitive NO donor) derivative conjugated with poly(L-cysteine)<sub>20</sub>-poly(ethylene oxide)<sub>45</sub>(PC) to prepare polypeptide micelles (PNOC).<sup>238</sup> In order to obtain photosensitivity, PDA was coated on PNOC which converted the NIR light into local

heat for the generation of both NO and PTT (Fig. 12C–E). In addition, DOX was used in a triple synergistic treatment strategy (PTT, NO gas therapy, and chemotherapy). After intravenous injection of the nanocomposite, the experimental results showed a remarkable 1 + 1 + 1 > 3 anticancer effect.

Heat energy also plays a dominant role in biochemical reactions, for example, it can induce heat-shock element (HSE) to turn the active trimers from inactive monomers for binding to the Hsp70 promoter and subsequent transcription. Inspired by this, a photothermal strategy for gene therapy based on the Hsp70 promoter was proposed.<sup>239</sup> Pin's group developed a NIR-II light-controlled genome editing nanosystem using the Hsp70 promoter-driven Cas9 plasmid.<sup>240</sup> In the system, a cationic polymer-coated Au nanorod assisted the gene delivery and served as a PTA to activate the HSP70 promoter, which promoted the expression of Cas9 under NIR-II light irradiation (Fig. 12F). This photogenetic switch to regulate gene expression has been proved for therapeutic genome editing *in vivo* with deep tissue-penetration and high spatial specificity and demonstrated high potential for broader applications.

### 4.3 Photomechanically triggered nanomedicine

Activation-engineered synthetic nanomaterials as nanodevices (nanorobots) provide a development direction for sophisticated tasks in nanomedicine.<sup>241</sup> Furthermore, as a non-invasive approach, light can trigger their autonomous motion by self-electrophoresis, self-diffusiophoresis, or self-thermophoresis.<sup>241</sup> However, self-electrophoresis and self-diffusiophoresis of nanorobots typically require high energy, *i.e.*, UV light, and thus self-thermophoresis seems to be more suitable for the fabrication of NIR light-triggered nanodevices. As such, He's group designed a NIR light-powered nanomotor (termed JMSNM) to integrate the functions of active seeking and membrane perforation for targeted therapy<sup>242</sup> (Fig. 13). The nanomotor was composed of a thick Au half-shell and mesoporous silica which was cloaked with a macrophage cell membrane (MPCM). Upon 808 nm irradiation, remarkable

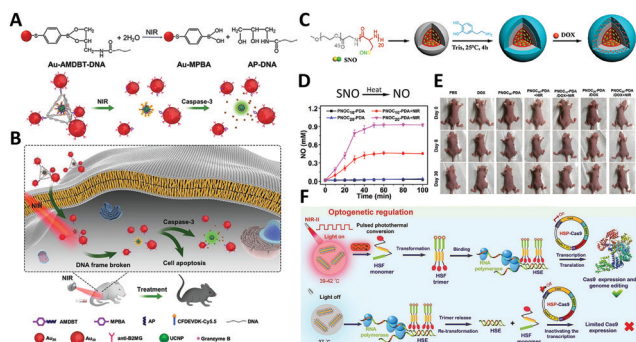


**Fig. 12** Photothermal chemistry for cancer therapy. (A) The design of NIR-induced disassembly of UAuTe tetrahedrons; in this system, AMDBT on Au nanoparticles can be decomposed into (4-mercaptophenyl) boronic acid (MPBA) and 3-amino-1,2-propanediol (AP) with the assistance of NIR laser irradiation (980 nm, 100  $\mu\text{J pulse}^{-1}$ , 50 Hz, 5 min). (B) Working mechanism of NIR light-controlled senescence clearance and apoptosis tracking by UAuTe tetrahedrons *in vivo*; reproduced with permission from ref. 234. Copyright 2020 Wiley-VCH. (C) Fabrication route of the PNOC-PDA nanocomposite. (D) NO-release curves of PNOC-PDA (1.0 mg mL<sup>-1</sup>). (E) Photographs of various tumors in each group; reproduced with permission from ref. 238. Copyright 2019 American Chemical Society. (F) Schematic illustration of the NIR-II optogenetic regulation of genome editing. Reproduced with permission from ref. 240.

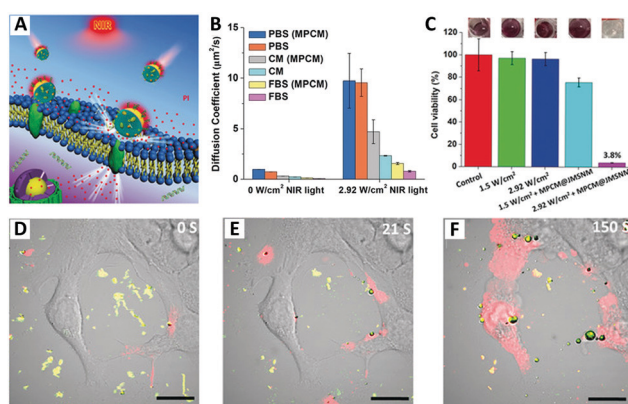


**Fig. 13** NIR photomechanically triggered nanomedicine. (A) Schematic illustration of MPCM@JMSNMs perforating the cell membranes under the assistance of NIR irradiation. (B) The diffusion coefficient of MPCM@JMSNMs in each group. (C) The therapeutic efficacy after different treatments detected by MTT. (D–F) The process of MPCM@JMSNMs perforating the cancer cell membranes. Power of NIR light = 2.92 W cm<sup>-2</sup>; scale bar: 20  $\mu\text{m}$ . Reproduced with permission from ref. 242. Copyright 2018 Wiley-VCH.

photothermal conversion of the Au half-shells led to a self-thermophoretic force that realized the directional movement of JMSNM. Additionally, the results demonstrated that subsequent illumination with NIR could assist MPCM@JMSNMs in photo-mechanically opening the cell membrane, which may pave the way for the application of self-propelled motors in the biomedical field. Besides, they further designed an ultrasound-driven gold-nanoshell-functionalized polymer multilayer tubular nanoswimmer to perforate the membrane of the targeted cell through a similar strategy.<sup>243</sup> The nanoswimmers could achieve the directional motion toward target cells with the assistance of ultrasound. After attachment onto the cells, the nanorobots opened the cell membrane within 0.1 s through the manipulation of NIR light owing to the high instantaneous photothermal effect of the Au shell. Such NIR-light-assisted nanodevices provided a considerable possibility for not only drug delivery, but also complex tasks in nanomedicine.

Another kind of Au-coated mechanoresponsive nanovesicle was fabricated for on-demand delivery of a drug in deep brain regions by Xiong *et al.*<sup>244</sup> This nanovesicle was prepared using an artificial phospholipid Rad-PC-Rad-based liposome whose mechanoresponsive characterization has been recognized in an early report. After cloaking with Au, NIR light could damage the nanostructure and release the drug due to the nanomechanical stress from the Au shell in sub-seconds. To verify the feasibility, the authors stereotaxically injected the calcein-loaded nanovesicle at different depths in deep brain regions of C57BL/6 mice. They found that NIR light triggered drug release even at 4 mm in the brain. This promising tool opened the door to optical manipulation of functional molecules in deep tissues for broad applications, such as cancer treatment and brain modulation.

## 5. Conclusion and perspectives

In this review, we summarized recent advances in NIR light-activated nanomedicine based on three main mechanisms: NIR-to-ROS conversion, upconversion activation, and the photothermal effect. During the past few decades, photoactive nanomedicine has been of considerable interest in precision therapy, especially tissue-penetration NIR monitoring. As is well known, NIR light-activated nanomedicine stands out for its deep penetration depth. Compared with other stimuli, this light demonstrates lower toxicity and highly specific spatiotemporal resolution, and has been widely used for generating chemical reactions or physical changes for targeted delivery or to direct tumor ablation using a nanomaterial transducer.

Beyond the aforementioned application of cancer therapy, additional directions of NIR light-activated nanomedicine should be included, *i.e.*, *in vivo* imaging, treatment of other diseases, and so on. Compared with visible light, NIR light circumvents the concern of relatively high signal-to-background ratios, phototoxicity, and limited penetration depths, which was widely explored during the past decade.<sup>2,202</sup> Besides, the emergence of NIR optogenetics provided a pioneering avenue to monitor and modulate the cell function in a spatiotemporal manner.<sup>1</sup> For instance, Wang *et al.* have designed a nanoplatfom with pre-inactivated DNA

agonist cloaking for regulating intracellular gene transcription.<sup>245</sup> In the system, localized photothermal stimulation mediated by AuNRs can activate DNA agonists for binding-induced dimerization of receptor tyrosine kinase (RTK) and downstream signal transduction. As previously reported, there exist some transmembrane protein complexes that are sensitive to light, which inspired the development of UCNP-based photogenetics for stem cell regulation and neuromodulation. In 2018, Chen *et al.* developed molecularly tailored UCNPs to evoke dopamine release in deep brain tissue.<sup>246</sup> Their results displayed the achievement of brain oscillations and silenced seizures *via* such strategies, suggesting the potential of NIR light-mediated neuronal control and neurological disorder therapies including for Alzheimer's and Parkinson's diseases. A large number of research studies claimed that the application of NIR based nanomedicine is also available for other disorders, such as genetic, cardiovascular, and metabolic diseases. In addition to therapy, an interesting NIR technology was demonstrated by Xian and his colleagues for achieving NIR light image vision.<sup>247</sup> They anchored the ocular photoreceptor-binding UCNPs on retinal photoreceptors as NIR light nanotransducers and endowed the injected mice with the ability to differentiate sophisticated NIR shape patterns. This strategy contributes to mammalian vision enhancement and may be employed for military applications.

Despite the described promise, there still exist a variety of challenges to clinical translation which need to be addressed. First, the toxicity of nanomaterials remains questionable. Up to now, researchers are mainly committed to developing late-model nanotechnology and demonstrate a simple proof of concept. The mechanism of clearance, accumulation profile, and chronic toxicity still remain quite unclear. Moreover, high time-consumption, high cost of production, and unstable product quality are usually encountered in the preparation of nanoformulations due to their relatively precise and complicated synthetic schemes. These drawbacks greatly increase the market risk of nanomedicine and dramatically limit their large-scale production for clinical use. Furthermore, most *in vivo* experiments of NIR light-activated nanomedicine were performed in preliminary studies. Current *in vivo* validations were mainly carried out through subcutaneous transplantation tumor models in mice as a proof of concept, and thus larger animal models (*i.e.*, pigs and monkeys) should be included as supplementary evidence to refine future nanomedicine clinical trials.

Overall, this photocontrolled nanomedicine has demonstrated great potential for broad applications beyond precision cancer therapy. Imaging, regenerative medicine, and more bioprocesses can also find inspiration from this strategy. Although long-term efforts should be made for conquering the above-mentioned challenges, current advances have sculpted an encouraging landscape of NIR light-activated nanomedicine and indicate that treatment strategies customized for individuals would become a forthcoming reality.

## Conflicts of interest

There are no conflicts to declare.

## Acknowledgements

This research was supported by the National Key R&D Program of China (2019YFA0709200), the National Natural Science Foundation of China (21874066 and 81601632), the Natural Science Foundation of Jiangsu Province (BK20160616 and BK20200336), the Fundamental Research Funds for Central Universities, and the Post-graduate Research & Practice Innovation Program of Jiangsu Province (KYCX20\_0036).

## References

- G. Chen, Y. Cao, Y. Tang, X. Yang, Y. Liu, D. Huang, Y. Zhang, C. Li and Q. Wang, Advanced near-infrared light for monitoring and modulating the spatiotemporal dynamics of cell functions in living systems, *Adv. Sci.*, 2020, **7**, 1903783.
- J. Son, G. Yi, J. Yoo, C. Park, H. Koo and H. S. Choi, Light-responsive nanomedicine for biophotonic imaging and targeted therapy, *Adv. Drug Delivery Rev.*, 2019, **138**, 133–147.
- B. Del Rosal, B. Jia and D. Jaque, Beyond phototherapy: Recent advances in multifunctional fluorescent nanoparticles for light-triggered tumor theranostics, *Adv. Funct. Mater.*, 2018, **28**, 1803733.
- Q. Xiong, Y. Lim, D. Li, K. Pu, L. Liang and H. Duan, Photoactive nanocarriers for controlled delivery, *Adv. Funct. Mater.*, 2020, **30**, 1903896.
- R. Vankayala and K. C. Hwang, Near-infrared-light-activatable nanomaterial-mediated phototheranostic nanomedicines: An emerging paradigm for cancer treatment, *Adv. Mater.*, 2018, **30**, 1706320.
- J. Yang, C. Wang, X. Liu, Y. Yin, Y.-H. Ma, Y. Gao, Y. Wang, Z. Lu and Y. Song, Gallium-carbenicillin framework coated defect-rich hollow TiO<sub>2</sub> as a photocatalyzed oxidative stress amplifier against complex infections, *Adv. Funct. Mater.*, 2020, **30**, 2004861.
- X. Xue, A. Lindstrom and Y. Li, Porphyrin-based nanomedicines for cancer treatment, *Bioconjugate Chem.*, 2019, **30**, 1585–1603.
- G. Chen, H. Qiu, P. N. Prasad and X. Chen, Upconversion nanoparticles: Design, nanochemistry, and applications in theranostics, *Chem. Rev.*, 2014, **114**, 5161–5214.
- M. L. Brongersma, N. J. Halas and P. Nordlander, Plasmon-induced hot carrier science and technology, *Nat. Nanotechnol.*, 2015, **10**, 25–34.
- Y. Min, J. M. Caster, M. J. Eblan and A. Z. Wang, Clinical translation of nanomedicine, *Chem. Rev.*, 2015, **115**, 11147–11190.
- V. Wagner, A. Dullaart, A.-K. Bock and A. Zweck, The emerging nanomedicine landscape, *Nat. Biotechnol.*, 2006, **24**, 1211–1217.
- R. van der Meel, E. Sulheim, Y. Shi, F. Kiessling, W. J. M. Mulder and T. Lammers, Smart cancer nanomedicine, *Nat. Nanotechnol.*, 2019, **14**, 1007–1017.
- B. Yang, Y. Chen and J. Shi, Reactive oxygen species (ROS)-based nanomedicine, *Chem. Rev.*, 2019, **119**, 4881–4985.
- Y. Yin, J. Yang, Y. Pan, Y. Gao, L. Huang, X. Luan, Z. Lin, W. Zhu, Y. Li and Y. Song, Mesopore to macropore transformation of metal-organic framework for drug delivery in inflammatory bowel disease, *Adv. Healthcare Mater.*, 2021, **10**, 2000973.
- X. Luan, Y. Pan, D. Zhou, B. He, X. Liu, Y. Gao, J. Yang and Y. Song, Cerium metal organic framework mediated molecular threading for point-of-care colorimetric assays, *Biosens. Bioelectron.*, 2020, **165**, 112406.
- M. Kendall and I. Lynch, Long-term monitoring for nanomedicine implants and drugs, *Nat. Nanotechnol.*, 2016, **11**, 206–210.
- S. Pandit, D. Dutta and S. Nie, Active transcytosis and new opportunities for cancer nanomedicine, *Nat. Mater.*, 2020, **19**, 478–480.
- P. D. Ramírez-García, J. S. Retamal, P. Shenoy, W. Imlach, M. Sykes, N. Truong, L. Constandil, T. Pelissier, C. J. Nowell, S. Y. Khor, L. M. Layani, C. Lumb, D. P. Poole, T. Lieu, G. D. Stewart, Q. N. Mai, D. D. Jensen, R. Latorre, N. N. Scheff, B. L. Schmidt, J. F. Quinn, M. R. Whittaker, N. A. Veldhuis, T. P. Davis and N. W. Bunnett, A pH-responsive nanoparticle targets the neurokinin 1 receptor in endosomes to prevent chronic pain, *Nat. Nanotechnol.*, 2019, **14**, 1150–1159.
- D. S. H. Wong, J. Li, X. Yan, B. Wang, R. Li, L. Zhang and L. Bian, Magnetically tuning tether mobility of integrin ligand regulates adhesion, spreading, and differentiation of stem cells, *Nano Lett.*, 2017, **17**, 1685–1695.
- Y. Zhang, J. Yu, H. N. Bomba, Y. Zhu and Z. Gu, Mechanical force-triggered drug delivery, *Chem. Rev.*, 2016, **116**, 12536–12563.
- M. Z. Alyami, S. K. Alsaiari, Y. Li, S. S. Qutub, F. A. Aleisa, R. Sougrat, J. S. Merzaban and N. M. Khashab, Cell-type-specific CRISPR/Cas9 delivery by biomimetic metal organic frameworks, *J. Am. Chem. Soc.*, 2020, **142**, 1715–1720.
- P. Zhang, D. Gao, K. An, Q. Shen, C. Wang, Y. Zhang, X. Pan, X. Chen, Y. Lyv, C. Cui, T. Liang, X. Duan, J. Liu, T. Yang, X. Hu, J.-J. Zhu, F. Xu and W. Tan, A programmable polymer library that enables the construction of stimuli-responsive nanocarriers containing logic gates, *Nat. Chem.*, 2020, **12**, 381–390.
- S. Yang, M. K. Shim, W. J. Kim, J. Choi, G.-H. Nam, J. Kim, J. Kim, Y. Moon, H. Y. Kim, J. Park, Y. Park, I.-S. Kim, J. H. Ryu and K. Kim, Cancer-activated doxorubicin pro-drug nanoparticles induce preferential immune response with minimal doxorubicin-related toxicity, *Biomaterials*, 2021, **272**, 120791.
- S. Mura, J. Nicolas and P. Couvreur, Stimuli-responsive nanocarriers for drug delivery, *Nat. Mater.*, 2013, **12**, 991–1003.
- Z. S. Al-Ahmady, W. T. Al-Jamal, J. V. Bossche, T. T. Bui, A. F. Drake, A. J. Mason and K. Kostarelos, Lipid-peptide vesicle nanoscale hybrids for triggered drug release by mild hyperthermia *in vitro* and *in vivo*, *ACS Nano*, 2012, **6**, 9335–9346.
- M.-Y. Hua, H.-L. Liu, H.-W. Yang, P.-Y. Chen, R.-Y. Tsai, C.-Y. Huang, I. C. Tseng, L.-A. Lyu, C.-C. Ma, H.-J. Tang,

- T.-C. Yen and K.-C. Wei, The effectiveness of a magnetic nanoparticle-based delivery system for BCNU in the treatment of gliomas, *Biomaterials*, 2011, **32**, 516–527.
- 27 S. Huo, P. Zhao, Z. Shi, M. Zou, X. Yang, E. Warszawik, M. Loznik, R. Göstl and A. Herrmann, Mechanochemical bond scission for the activation of drugs, *Nat. Chem.*, 2021, **13**, 131–139.
- 28 N. S. Awad, V. Paul, N. M. AlSawaftah, G. ter Haar, T. M. Allen, W. G. Pitt and G. A. Hussein, Ultrasound-responsive nanocarriers in cancer treatment: A review, *ACS Pharmacol. Transl. Sci.*, 2021, **4**, 589–612.
- 29 W. Zhao, Y. Zhao, Q. Wang, T. Liu, J. Sun and R. Zhang, Remote light-responsive nanocarriers for controlled drug delivery: Advances and perspectives, *Small*, 2019, **15**, 1903060.
- 30 X. Zhu, X. Ji, N. Kong, Y. Chen, M. Mahmoudi, X. Xu, L. Ding, W. Tao, T. Cai, Y. Li, T. Gan, A. Barrett, Z. Bharwani, H. Chen and O. C. Farokhzad, Intracellular mechanistic understanding of 2D MoS<sub>2</sub> nanosheets for anti-exocytosis-enhanced synergistic cancer therapy, *ACS Nano*, 2018, **12**, 2922–2938.
- 31 W. Fan, P. Huang and X. Chen, Overcoming the Achilles' heel of photodynamic therapy, *Chem. Soc. Rev.*, 2016, **45**, 6488–6519.
- 32 P. Juzenas, A. Juzeniene, O. Kaalhus, V. Iani and J. Moan, Noninvasive fluorescence excitation spectroscopy during application of 5-aminolevulinic acid *in vivo*, *Photochem. Photobiol. Sci.*, 2002, **1**, 745–748.
- 33 I. J. Macdonald and T. J. Dougherty, Basic principles of photodynamic therapy, *J. Porphyrins Phthalocyanines*, 2001, **05**, 105–129.
- 34 K. Plaetzer, B. Krammer, J. Berlanda, F. Berr and T. Kiesslich, Photophysics and photochemistry of photodynamic therapy: Fundamental aspects, *Lasers Med. Sci.*, 2009, **24**, 259–268.
- 35 M. Li, Y. Shao, J. H. Kim, Z. Pu, X. Zhao, H. Huang, T. Xiong, Y. Kang, G. Li, K. Shao, J. Fan, J. W. Foley, J. S. Kim and X. Peng, Unimolecular photodynamic O<sub>2</sub>-economizer to overcome hypoxia resistance in phototherapeutics, *J. Am. Chem. Soc.*, 2020, **142**, 5380–5388.
- 36 M. Li, T. Xiong, J. Du, R. Tian, M. Xiao, L. Guo, S. Long, J. Fan, W. Sun, K. Shao, X. Song, J. W. Foley and X. Peng, Superoxide radical photogenerator with amplification effect: Surmounting the Achilles' Heels of photodynamic oncotherapy, *J. Am. Chem. Soc.*, 2019, **141**, 2695–2702.
- 37 M. Li, J. Xia, R. Tian, J. Wang, J. Fan, J. Du, S. Long, X. Song, J. W. Foley and X. Peng, Near-infrared light-initiated molecular superoxide radical generator: Rejuvenating photodynamic therapy against hypoxic tumors, *J. Am. Chem. Soc.*, 2018, **140**, 14851–14859.
- 38 K. Zhang, Z. Yu, X. Meng, W. Zhao, Z. Shi, Z. Yang, H. Dong and X. Zhang, A bacteriochlorin-based metal–organic framework nanosheet superoxide radical generator for photoacoustic imaging-guided highly efficient photodynamic therapy, *Adv. Sci.*, 2019, **6**, 1900530.
- 39 G. Hong, A. L. Antaris and H. Dai, Near-infrared fluorophores for biomedical imaging, *Nat. Biomed. Eng.*, 2017, **1**, 0010.
- 40 A. L. Antaris, H. Chen, K. Cheng, Y. Sun, G. Hong, C. Qu, S. Diao, Z. Deng, X. Hu, B. Zhang, X. Zhang, O. K. Yaghi, Z. R. Alamparambil, X. Hong, Z. Cheng and H. Dai, A small-molecule dye for NIR-II imaging, *Nat. Mater.*, 2016, **15**, 235–242.
- 41 J. Chen, T. Fan, Z. Xie, Q. Zeng, P. Xue, T. Zheng, Y. Chen, X. Luo and H. Zhang, Advances in nanomaterials for photodynamic therapy applications: Status and challenges, *Biomaterials*, 2020, **237**, 119827.
- 42 C. C. Winterbourn, Reconciling the chemistry and biology of reactive oxygen species, *Nat. Chem. Biol.*, 2008, **4**, 278–286.
- 43 C. Nathan and A. Cunningham-Bussel, beyond oxidative stress: an immunologist's guide to reactive oxygen species, *Nat. Rev. Immunol.*, 2013, **13**, 349–361.
- 44 X. Li, N. Kwon, T. Guo, Z. Liu and J. Yoon, Innovative strategies for hypoxic-tumor photodynamic therapy, *Angew. Chem., Int. Ed.*, 2018, **57**, 11522–11531.
- 45 S.-Y. Yin, G. Song, Y. Yang, Y. Zhao, P. Wang, L.-M. Zhu, X. Yin and X.-B. Zhang, Persistent regulation of tumor microenvironment *via* circulating catalysis of MnFe<sub>2</sub>O<sub>4</sub>@metal–organic frameworks for enhanced photodynamic therapy, *Adv. Funct. Mater.*, 2019, **29**, 1901417.
- 46 D. Wang, H. Wu, S. Z. F. Phua, G. Yang, W. Qi Lim, L. Gu, C. Qian, H. Wang, Z. Guo, H. Chen and Y. Zhao, Self-assembled single-atom nanozyme for enhanced photodynamic therapy treatment of tumor, *Nat. Commun.*, 2020, **11**, 357.
- 47 Z. Yu, P. Zhou, W. Pan, N. Li and B. Tang, A biomimetic nanoreactor for synergistic chemiexcited photodynamic therapy and starvation therapy against tumor metastasis, *Nat. Commun.*, 2018, **9**, 5044.
- 48 Z. Wang, Y. Zhang, E. Ju, Z. Liu, F. Cao, Z. Chen, J. Ren and X. Qu, Biomimetic nanoflowers by self-assembly of nanozymes to induce intracellular oxidative damage against hypoxic tumors, *Nat. Commun.*, 2018, **9**, 3334.
- 49 S. Kang, Y.-G. Gil, D.-H. Min and H. Jang, Nonrecurring circuit nanozymatic enhancement of hypoxic pancreatic cancer phototherapy using speckled Ru–Te hollow nanorods, *ACS Nano*, 2020, **14**, 4383–4394.
- 50 L. He, Q. Ni, J. Mu, W. Fan, L. Liu, Z. Wang, L. Li, W. Tang, Y. Liu, Y. Cheng, L. Tang, Z. Yang, Y. Liu, J. Zou, W. Yang, O. Jacobson, F. Zhang, P. Huang and X. Chen, Solvent-assisted self-assembly of a metal–organic framework based biocatalyst for cascade reaction driven photodynamic therapy, *J. Am. Chem. Soc.*, 2020, **142**, 6822–6832.
- 51 Y. Yang, M. Chen, B. Wang, P. Wang, Y. Liu, Y. Zhao, K. Li, G. Song, X.-B. Zhang and W. Tan, NIR-II driven plasmon-enhanced catalysis for a timely supply of oxygen to overcome hypoxia-induced radiotherapy tolerance, *Angew. Chem., Int. Ed.*, 2019, **58**, 15069–15075.
- 52 Y. Zhang, F. Wang, C. Liu, Z. Wang, L. Kang, Y. Huang, K. Dong, J. Ren and X. Qu, Nanozyme decorated metal–organic frameworks for enhanced photodynamic therapy, *ACS Nano*, 2018, **12**, 651–661.
- 53 H. Cheng, J.-Y. Zhu, S.-Y. Li, J.-Y. Zeng, Q. Lei, K.-W. Chen, C. Zhang and X.-Z. Zhang, An O<sub>2</sub> self-sufficient biomimetic nanoplatform for highly specific and efficient photodynamic therapy, *Adv. Funct. Mater.*, 2016, **26**, 7847–7860.



- 54 Q. Chen, J. Chen, Z. Yang, L. Zhang, Z. Dong and Z. Liu, NIR-II light activated photodynamic therapy with protein-capped gold nanoclusters, *Nano Res.*, 2018, **11**, 5657–5669.
- 55 S.-Y. Li, H. Cheng, B.-R. Xie, W.-X. Qiu, J.-Y. Zeng, C.-X. Li, S.-S. Wan, L. Zhang, W.-L. Liu and X.-Z. Zhang, Cancer cell membrane camouflaged cascade bioreactor for cancer targeted starvation and photodynamic therapy, *ACS Nano*, 2017, **11**, 7006–7018.
- 56 J. Wu, X. Wang, Q. Wang, Z. Lou, S. Li, Y. Zhu, L. Qin and H. Wei, Nanomaterials with enzyme-like characteristics (nanozymes): Next-generation artificial enzymes(II), *Chem. Soc. Rev.*, 2019, **48**, 1004–1076.
- 57 Y. Sang, F. Cao, W. Li, L. Zhang, Y. You, Q. Deng, K. Dong, J. Ren and X. Qu, Bioinspired construction of a nanozyme-based H<sub>2</sub>O<sub>2</sub> homeostasis disruptor for intensive chemodynamic therapy, *J. Am. Chem. Soc.*, 2020, **142**, 5177–5183.
- 58 Y. Lin, Z. Chen and X. Y. Liu, Using inorganic nanomaterials to endow biocatalytic systems with unique features, *Trends Biotechnol.*, 2016, **34**, 303–315.
- 59 M. Liang and X. Yan, Nanozymes: From new concepts, mechanisms, and standards to applications, *Acc. Chem. Res.*, 2019, **52**, 2190–2200.
- 60 X. Liu, Y. Pan, J. Yang, Y. Gao, T. Huang, X. Luan, Y. Wang and Y. Song, Gold nanoparticles doped metal-organic frameworks as near-infrared light-enhanced cascade nanozyme against hypoxic tumors, *Nano Res.*, 2020, **13**, 653–660.
- 61 M. Diehn, R. W. Cho, N. A. Lobo, T. Kalisky, M. J. Dorie, A. N. Kulp, D. Qian, J. S. Lam, L. E. Ailles, M. Wong, B. Joshua, M. J. Kaplan, I. Wapnir, F. M. Dirbas, G. Somlo, C. Garberoglio, B. Paz, J. Shen, S. K. Lau, S. R. Quake, J. M. Brown, I. L. Weissman and M. F. Clarke, Association of reactive oxygen species levels and radioresistance in cancer stem cells, *Nature*, 2009, **458**, 780–783.
- 62 H. Min, J. Wang, Y. Qi, Y. Zhang, X. Han, Y. Xu, J. Xu, Y. Li, L. Chen, K. Cheng, G. Liu, N. Yang, Y. Li and G. Nie, Biomimetic metal-organic framework nanoparticles for cooperative combination of antiangiogenesis and photodynamic therapy for enhanced efficacy, *Adv. Mater.*, 2019, **31**, 1808200.
- 63 C.-K. Lim, J. Heo, S. Shin, K. Jeong, Y. H. Seo, W.-D. Jang, C. R. Park, S. Y. Park, S. Kim and I. C. Kwon, Nanophotosensitizers toward advanced photodynamic therapy of Cancer, *Cancer Lett.*, 2013, **334**, 176–187.
- 64 S.-S. Wan, Q. Cheng, X. Zeng and X.-Z. Zhang, A Mn(III)-sealed metal-organic framework nanosystem for redox-unlocked tumor theranostics, *ACS Nano*, 2019, **13**, 6561–6571.
- 65 G. Yang, L. Xu, Y. Chao, J. Xu, X. Sun, Y. Wu, R. Peng and Z. Liu, Hollow MnO<sub>2</sub> as a tumor-microenvironment-responsive biodegradable nano-platform for combination therapy favoring antitumor immune responses, *Nat. Commun.*, 2017, **8**, 902.
- 66 H. Fan, Z. Zhao, G. Yan, X. Zhang, C. Yang, H. Meng, Z. Chen, H. Liu and W. Tan, A smart DNAzyme-MnO<sub>2</sub> nanosystem for efficient gene silencing, *Angew. Chem., Int. Ed.*, 2015, **54**, 4801–4805.
- 67 H. Fan, G. Yan, Z. Zhao, X. Hu, W. Zhang, H. Liu, X. Fu, T. Fu, X.-B. Zhang, W. Tan and A. Smart, Photosensitizer-manganese dioxide nanosystem for enhanced photodynamic therapy by reducing glutathione levels in cancer cells, *Angew. Chem., Int. Ed.*, 2016, **55**, 5477–5482.
- 68 W. Zhang, J. Lu, X. Gao, P. Li, W. Zhang, Y. Ma, H. Wang and B. Tang, Enhanced photodynamic therapy by reduced levels of intracellular glutathione obtained by employing a nano-MOF with CuII as the active center, *Angew. Chem., Int. Ed.*, 2018, **57**, 4891–4896.
- 69 Z. Zhang, R. Wang, X. Huang, R. Luo, J. Xue, J. Gao, W. Liu, F. Liu, F. Feng and W. Qu, Self-delivered and self-monitored chemo-photodynamic nanoparticles with light-triggered synergistic antitumor therapies by downregulation of HIF-1 $\alpha$  and depletion of GSH, *ACS Appl. Mater. Interfaces*, 2020, **12**, 5680–5694.
- 70 M. Pan, Q. Jiang, J. Sun, Z. Xu, Y. Zhou, L. Zhang and X. Liu, Programming DNA nanoassembly for enhanced photodynamic therapy, *Angew. Chem., Int. Ed.*, 2020, **59**, 1897–1905.
- 71 M. Broekgaarden, R. Weijer, M. Krekorian, B. van den Ijssel, M. Kos, L. K. Alles, A. C. van Wijk, Z. Bikadi, E. Hazai, T. M. van Gulik and M. Heger, Inhibition of hypoxia-inducible factor 1 with acriflavine sensitizes hypoxic tumor cells to photodynamic therapy with zinc phthalocyanine-encapsulating cationic liposomes, *Nano Res.*, 2016, **9**, 1639–1662.
- 72 L. Zhao, J. Li, Y. Su, L. Yang, L. Chen, L. Qiang, Y. Wang, H. Xiang, H. P. Tham, J. Peng and Y. Zhao, MTH1 inhibitor amplifies the lethality of reactive oxygen species to tumor in photodynamic therapy, *Sci. Adv.*, 2020, **6**, eaaz0575.
- 73 L.-P. Zhao, R.-R. Zheng, H.-Q. Chen, L.-S. Liu, X.-Y. Zhao, H.-H. Liu, X.-Z. Qiu, X.-Y. Yu, H. Cheng and S.-Y. Li, Self-delivery nanomedicine for O<sub>2</sub>-economized photodynamic tumor therapy, *Nano Lett.*, 2020, **20**, 2062–2071.
- 74 W. Zeng, P. Liu, W. Pan, S. R. Singh and Y. Wei, Hypoxia and hypoxia inducible factors in tumor metabolism, *Cancer Lett.*, 2015, **356**, 263–267.
- 75 S.-B. Wang, Z.-X. Chen, F. Gao, C. Zhang, M.-Z. Zou, J.-J. Ye, X. Zeng and X.-Z. Zhang, Remodeling extracellular matrix based on functional covalent organic framework to enhance tumor photodynamic therapy, *Biomaterials*, 2020, **234**, 119772.
- 76 X. Zhao, S. Long, M. Li, J. Cao, Y. Li, L. Guo, W. Sun, J. Du, J. Fan and X. Peng, Oxygen-dependent regulation of excited-state deactivation process of rational photosensitizer for smart phototherapy, *J. Am. Chem. Soc.*, 2020, **142**, 1510–1517.
- 77 N. Kong, X. Ji, J. Wang, X. Sun, G. Chen, T. Fan, W. Liang, H. Zhang, A. Xie, O. C. Farokhzad and W. Tao, ROS-mediated selective killing effect of black phosphorus: Mechanistic understanding and its guidance for safe biomedical applications, *Nano Lett.*, 2020, **20**, 3943–3955.
- 78 N. M. Idris, M. K. Gnanasammandhan, J. Zhang, P. C. Ho, R. Mahendran and Y. Zhang, *In vivo* photodynamic therapy using upconversion nanoparticles as remote-controlled nanotransducers, *Nat. Med.*, 2012, **18**, 1580–1585.
- 79 Y. Wang, N. Gong, Y. Li, Q. Lu, X. Wang and J. Li, Atomic-level nanorings (A-NRs) therapeutic agent for photoacoustic imaging and photothermal/photodynamic therapy of cancer, *J. Am. Chem. Soc.*, 2020, **142**, 1735–1739.

- 80 L. Shi, F. Hu, Y. Duan, W. Wu, J. Dong, X. Meng, X. Zhu and B. Liu, Hybrid nanospheres to overcome hypoxia and intrinsic oxidative resistance for enhanced photodynamic therapy, *ACS Nano*, 2020, **14**, 2183–2190.
- 81 H. Wang, D. Yu, J. Fang, C. Cao, Z. Liu, J. Ren and X. Qu, Renal-clearable porphyrinic metal–organic framework nanodots for enhanced photodynamic therapy, *ACS Nano*, 2019, **13**, 9206–9217.
- 82 B. Zhao, Y. Wang, X. Yao, D. Chen, M. Fan, Z. Jin and Q. He, Photocatalysis-mediated drug-free sustainable cancer therapy using nanocatalyst, *Nat. Commun.*, 2021, **12**, 1345.
- 83 J. Li and K. Pu, Semiconducting polymer nanomaterials as near-infrared photoactivatable protherapeutics for cancer, *Acc. Chem. Res.*, 2020, **53**, 752–762.
- 84 T. Sun, J. Han, S. Liu, X. Wang, Z. Y. Wang and Z. Xie, Tailor-made semiconducting polymers for second near-infrared photothermal therapy of orthotopic liver cancer, *ACS Nano*, 2019, **13**, 7345–7354.
- 85 C. Wu, T. Schneider, M. Zeigler, J. Yu, P. G. Schiro, D. R. Burnham, J. D. McNeill and D. T. Chiu, Bioconjugation of ultrabright semiconducting polymer dots for specific cellular targeting, *J. Am. Chem. Soc.*, 2010, **132**, 15410–15417.
- 86 J. Zou, J. Zhu, Z. Yang, L. Li, W. Fan, L. He, W. Tang, L. Deng, J. Mu, Y. Ma, Y. Cheng, W. Huang, X. Dong and X. Chen, A Phototheranostic Strategy to continuously deliver singlet oxygen in the dark and hypoxic tumor microenvironment, *Angew. Chem., Int. Ed.*, 2020, **59**, 8833–8838.
- 87 H. Wang, X. Pan, X. Wang, W. Wang, Z. Huang, K. Gu, S. Liu, F. Zhang, H. Shen, Q. Yuan, J. Ma, W. Yuan and H. Liu, Degradable carbon–silica nanocomposite with immunoadjuvant property for dual-modality photothermal/photodynamic therapy, *ACS Nano*, 2020, **14**, 2847–2859.
- 88 C. Yao, Y. Li, Z. Wang, C. Song, X. Hu and S. Liu, Cytosolic NQO1 enzyme-activated near-infrared fluorescence imaging and photodynamic therapy with polymeric vesicles, *ACS Nano*, 2020, **14**, 1919–1935.
- 89 K. Kim, C.-S. Lee and K. Na, Light-controlled reactive oxygen species (ROS)-producible polymeric micelles with simultaneous drug-release triggering and endo/lysosomal escape, *Chem. Commun.*, 2016, **52**, 2839–2842.
- 90 G. Saravanakumar and W. J. Kim, Light-induced reactive-oxygen-species- (ROS-) mediated activation of self-assembled nanoplatfoms for on-demand drug delivery, in *Targeted Nanosystems for Therapeutic Applications: New Concepts, Dynamic Properties, Efficiency, and Toxicity*, American Chemical Society, 2019, vol. 1309, pp. 253–285.
- 91 G. Saravanakumar, J. Lee, J. Kim and W. J. Kim, Visible light-induced singlet oxygen-mediated intracellular disassembly of polymeric micelles co-loaded with a photosensitizer and an anticancer drug for enhanced photodynamic therapy, *Chem. Commun.*, 2015, **51**, 9995–9998.
- 92 Y. Lyu, S. He, J. Li, Y. Jiang, H. Sun, Y. Miao and K. Pu, A photolabile semiconducting polymer nanotransducer for near-infrared regulation of CRISPR/Cas9 gene editing, *Angew. Chem., Int. Ed.*, 2019, **58**, 18197–18201.
- 93 Q. Yan, J. Hu, R. Zhou, Y. Ju, Y. Yin and J. Yuan, Visible light-responsive micelles formed from dialkoxanthracene-containing block copolymers, *Chem. Commun.*, 2012, **48**, 1913–1915.
- 94 G. Saravanakumar, H. Park, J. Kim, D. Park, S. Pramanick, D. H. Kim and W. J. Kim, Miktoarm amphiphilic block copolymer with singlet oxygen-labile stereospecific  $\beta$ -aminoacrylate junction: Synthesis, self-assembly, and photo-dynamically triggered drug release, *Biomacromolecules*, 2018, **19**, 2202–2213.
- 95 C. de Gracia Lux, S. Joshi-Barr, T. Nguyen, E. Mahmoud, E. Schopf, N. Fomina and A. Almutairi, Biocompatible polymeric nanoparticles degrade and release cargo in response to biologically relevant levels of hydrogen peroxide, *J. Am. Chem. Soc.*, 2012, **134**, 15758–15764.
- 96 Y. Wu, D. Zhou, Y. Qi, Z. Xie, X. Chen, X. Jing and Y. Huang, Novel multi-sensitive pseudo-poly(amino acid) for effective intracellular drug delivery, *RSC Adv.*, 2015, **5**, 31972–31983.
- 97 S. S. Yu, R. L. Koblin, A. L. Zachman, D. S. Perrien, L. H. Hofmeister, T. D. Giorgio and H.-J. Sung, Physiologically relevant oxidative degradation of oligo(proline) cross-linked polymeric scaffolds, *Biomacromolecules*, 2011, **12**, 4357–4366.
- 98 Z. Liu, T. Cao, Y. Xue, M. Li, M. Wu, J. W. Engle, Q. He, W. Cai, M. Lan and W. Zhang, Self-amplified photodynamic therapy through the  $^1\text{O}_2$ -mediated internalization of photosensitizers from a Ppa-bearing block copolymer, *Angew. Chem., Int. Ed.*, 2020, **59**, 3711–3717.
- 99 D. Jia, X. Ma, Y. Lu, X. Li, S. Hou, Y. Gao, P. Xue, Y. Kang and Z. Xu, ROS-responsive cyclodextrin nanoplatfom for combined photodynamic therapy and chemotherapy of cancer, *Chin. Chem. Lett.*, 2021, **32**, 162–167.
- 100 X. Shi, Y. Zhang, Y. Tian, S. Xu, E. Ren, S. Bai, X. Chen, C. Chu, Z. Xu and G. Liu, Multi-responsive Bottlebrush-like unimolecules self-assembled nano-riceball for synergistic sono-chemotherapy, *Small Methods*, 2021, **5**, 2000416.
- 101 Q. Li, W. Li, H. Di, L. Luo, C. Zhu, J. Yang, X. Yin, H. Yin, J. Gao, Y. Du and J. You, A photosensitive liposome with NIR light triggered doxorubicin release as a combined photodynamic-chemo therapy system, *J. Controlled Release*, 2018, **277**, 114–125.
- 102 Y. Wang, Y. Deng, H. Luo, A. Zhu, H. Ke, H. Yang and H. Chen, Light-responsive nanoparticles for highly efficient cytoplasmic delivery of anticancer agents, *ACS Nano*, 2017, **11**, 12134–12144.
- 103 A. Napoli, M. Valentini, N. Tirelli, M. Müller and J. A. Hubbell, Oxidation-responsive polymeric vesicles, *Nat. Mater.*, 2004, **3**, 183–189.
- 104 F. Li, T. Li, W. Cao, L. Wang and H. Xu, Near-infrared light stimuli-responsive synergistic therapy nanoplatfoms based on the coordination of tellurium-containing block polymer and cisplatin for cancer treatment, *Biomaterials*, 2017, **133**, 208–218.
- 105 B. Du, S. Jia, Q. Wang, X. Ding, Y. Liu, H. Yao and J. Zhou, A self-targeting, dual ROS/pH-responsive apoferritin nanocage for spatiotemporally controlled drug delivery to breast cancer, *Biomacromolecules*, 2018, **19**, 1026–1036.

- 106 J. Park, M. Xu, F. Li and H.-C. Zhou, 3D long-range triplet migration in a water-stable metal–organic framework for upconversion-based ultralow-power in vivo imaging, *J. Am. Chem. Soc.*, 2018, **140**, 5493–5499.
- 107 W. Li, J. Wang, J. Ren and X. Qu, Near-infrared upconversion controls photocaged cell adhesion, *J. Am. Chem. Soc.*, 2014, **136**, 2248–2251.
- 108 W. Li, Z. Chen, L. Zhou, Z. Li, J. Ren and X. Qu, Non-invasive and reversible cell adhesion and detachment via single-wavelength near-infrared laser mediated photoisomerization, *J. Am. Chem. Soc.*, 2015, **137**, 8199–8205.
- 109 Y. Li, X. Liu, X. Yang, H. Lei, Y. Zhang and B. Li, Enhancing upconversion fluorescence with a natural bio-microlens, *ACS Nano*, 2017, **11**, 10672–10680.
- 110 X. Zhu, J. Li, X. Qiu, Y. Liu, W. Feng and F. Li, Upconversion nanocomposite for programming combination cancer therapy by precise control of microscopic temperature, *Nat. Commun.*, 2018, **9**, 2176.
- 111 Q. Mei, A. Bansal, M. K. G. Jayakumar, Z. Zhang, J. Zhang, H. Huang, D. Yu, C. J. A. Ramachandra, D. J. Hausenloy, T. W. Soong and Y. Zhang, Manipulating energy migration within single lanthanide activator for switchable upconversion emissions towards bidirectional photoactivation, *Nat. Commun.*, 2019, **10**, 4416.
- 112 X. Xie, N. Gao, R. Deng, Q. Sun, Q.-H. Xu and X. Liu, Mechanistic investigation of photon upconversion in Nd<sup>3+</sup>-sensitized core–shell nanoparticles, *J. Am. Chem. Soc.*, 2013, **135**, 12608–12611.
- 113 X. Ai, C. J. H. Ho, J. Aw, A. B. E. Attia, J. Mu, Y. Wang, X. Wang, Y. Wang, X. Liu, H. Chen, M. Gao, X. Chen, E. K. L. Yeow, G. Liu, M. Olivo and B. Xing, *In vivo* covalent cross-linking of photon-converted rare-earth nanostructures for tumour localization and theranostics, *Nat. Commun.*, 2016, **7**, 10432.
- 114 B. Zhou, L. Yan, J. Huang, X. Liu, L. Tao and Q. Zhang, NIR II-responsive photon upconversion through energy migration in an ytterbium sublattice, *Nat. Photonics*, 2020, **14**, 760–766.
- 115 R. Song, H. Wang, M. Zhang, Y. Liu, X. Meng, S. Zhai, C.-C. Wang, T. Gong, Y. Wu, X. Jiang and W. Bu, Near-infrared light-triggered chlorine radical (<sup>•</sup>Cl) stress for cancer therapy, *Angew. Chem., Int. Ed.*, 2020, **59**, 21032–21040.
- 116 A. Zamora, G. Viguera, V. Rodríguez, M. D. Santana and J. Ruiz, Cyclometalated iridium(III) luminescent complexes in therapy and phototherapy, *Coord. Chem. Rev.*, 2018, **360**, 34–76.
- 117 J. Zhao, X. Zhang, L. Fang, C. Gao, C. Xu and S. Gou, Iridium(III) complex-derived polymeric micelles with low dark toxicity and strong NIR excitation for phototherapy and chemotherapy, *Small*, 2020, **16**, 2000363.
- 118 L. Wang and Q. Li, Photochromism into nanosystems: towards lighting up the future nanoworld, *Chem. Soc. Rev.*, 2018, **47**, 1044–1097.
- 119 M. Karimi, P. Sahandi Zangabad, S. Baghaee-Ravari, M. Ghazadeh, H. Mirshekari and M. R. Hamblin, Smart nanostructures for cargo delivery: Uncaging and activating by light, *J. Am. Chem. Soc.*, 2017, **139**, 4584–4610.
- 120 J. Liu, W. Bu, L. Pan and J. Shi, NIR-triggered anticancer drug delivery by upconverting nanoparticles with integrated azobenzene-modified mesoporous silica, *Angew. Chem., Int. Ed.*, 2013, **52**, 4375–4379.
- 121 W.-L. Wan, B. Tian, Y.-J. Lin, C. Korupalli, M.-Y. Lu, Q. Cui, D. Wan, Y. Chang and H.-W. Sung, Photosynthesis-inspired H<sub>2</sub> generation using a chlorophyll-loaded liposomal nanoplatform to detect and scavenge excess ROS, *Nat. Commun.*, 2020, **11**, 534.
- 122 H. Chen, X. Zeng, H. P. Tham, S. Z. F. Phua, W. Cheng, W. Zeng, H. Shi, L. Mei and Y. Zhao, NIR-light-activated combination therapy with a precise ratio of photosensitizer and prodrug using a host–guest strategy, *Angew. Chem., Int. Ed.*, 2019, **58**, 7641–7646.
- 123 H. M. D. Bandara and S. C. Burdette, Photoisomerization in different classes of azobenzene, *Chem. Soc. Rev.*, 2012, **41**, 1809–1825.
- 124 Y. Wang, Y. Han, X. Tan, Y. Dai, F. Xia and X. Zhang, Cyclodextrin capped gold nanoparticles (AuNP@CDs): From synthesis to applications, *J. Mater. Chem. B*, 2021, **9**, 2584–2593.
- 125 C. Yao, P. Wang, X. Li, X. Hu, J. Hou, L. Wang and F. Zhang, Near-infrared-triggered azobenzene-liposome/upconversion nanoparticle hybrid vesicles for remotely controlled drug delivery to overcome cancer multidrug resistance, *Adv. Mater.*, 2016, **28**, 9341–9348.
- 126 Y. Zhang, Y. Zhang, G. Song, Y. He, X. Zhang, Y. Liu and H. Ju, A DNA–azobenzene nanopump fueled by upconversion luminescence for controllable intracellular drug release, *Angew. Chem., Int. Ed.*, 2019, **58**, 18207–18211.
- 127 H. Zhao, E. S. Sterner, E. B. Coughlin and P. Theato, *o*-Nitrobenzyl alcohol derivatives: Opportunities in polymer and materials science, *Macromolecules*, 2012, **45**, 1723–1736.
- 128 Z. Yan, H. Qin, J. Ren and X. Qu, Photocontrolled multidirectional differentiation of mesenchymal stem cells on an upconversion substrate, *Angew. Chem., Int. Ed.*, 2018, **57**, 11182–11187.
- 129 Y. Fatiev, J. G. Croissant, S. Alsaiari, B. A. Moosa, D. H. Anjum and N. M. Khashab, Photoresponsive bridged silsesquioxane nanoparticles with tunable morphology for light-triggered plasmid DNA delivery, *ACS Appl. Mater. Interfaces*, 2015, **7**, 24993–24997.
- 130 L. Yang, H. Sun, Y. Liu, W. Hou, Y. Yang, R. Cai, C. Cui, P. Zhang, X. Pan, X. Li, L. Li, B. S. Sumerlin and W. Tan, Self-assembled aptamer-grafted hyperbranched polymer nanocarrier for targeted and photoresponsive drug delivery, *Angew. Chem., Int. Ed.*, 2018, **57**, 17048–17052.
- 131 Y. Pan, J. Yang, X. Luan, X. Liu, X. Li, J. Yang, T. Huang, L. Sun, Y. Wang, Y. Lin and Y. Song, Near-infrared upconversion-activated CRISPR-Cas9 system: A remote-controlled gene editing platform, *Sci. Adv.*, 2019, **5**, eaav7199.
- 132 M. Zhou, H. Huang, D. Wang, H. Lu, J. Chen, Z. Chai, S. Q. Yao and Y. Hu, Light-triggered PEGylation/dePEGylation of the nanocarriers for enhanced tumor penetration, *Nano Lett.*, 2019, **19**, 3671–3675.
- 133 H. Chu, J. Zhao, Y. Mi, Z. Di and L. Li, NIR-light-mediated spatially selective triggering of anti-tumor immunity via

- upconversion nanoparticle-based immunodevices, *Nat. Commun.*, 2019, **10**, 2839.
- 134 A. Albert, Chemical aspects of selective toxicity, *Nature*, 1958, **182**, 421–423.
- 135 J. Rautio, N. A. Meanwell, L. Di and M. J. Hageman, The expanding role of prodrugs in contemporary drug design and development, *Nat. Rev. Drug Discovery*, 2018, **17**, 559–587.
- 136 M. T. Jarlstad Olesen, R. Walther, P. P. Poier, F. Dagnæs-Hansen and A. N. Zelikin, Molecular, macromolecular, and supramolecular glucuronide prodrugs: Lead identified for anticancer prodrug monotherapy, *Angew. Chem., Int. Ed.*, 2020, **59**, 7390–7396.
- 137 S. Xu, X. Zhu, C. Zhang, W. Huang, Y. Zhou and D. Yan, Oxygen and Pt(II) self-generating conjugate for synergistic photo-chemo therapy of hypoxic tumor, *Nat. Commun.*, 2018, **9**, 2053.
- 138 S. H. C. Askes and S. Bonnet, Solving the oxygen sensitivity of sensitized photon upconversion in life science applications, *Nat. Rev. Chem.*, 2018, **2**, 437–452.
- 139 L. Chen, S.-F. Zhou, L. Su and J. Song, Gas-mediated cancer bioimaging and therapy, *ACS Nano*, 2019, **13**, 10887–10917.
- 140 C. Hu, X. Cun, S. Ruan, R. Liu, W. Xiao, X. Yang, Y. Yang, C. Yang and H. Gao, Enzyme-triggered size shrink and laser-enhanced NO release nanoparticles for deep tumor penetration and combination therapy, *Biomaterials*, 2018, **168**, 64–75.
- 141 X. Zhang, Y. Liu, S. Gopalakrishnan, L. Castellanos-Garcia, G. Li, M. Malassiné, I. Uddin, R. Huang, D. C. Luther, R. W. Vachet and V. M. Rotello, Intracellular activation of bioorthogonal nanozymes through endosomal proteolysis of the protein corona, *ACS Nano*, 2020, **14**, 4767–4773.
- 142 Q. Zhang, G. Kuang, S. He, H. Lu, Y. Cheng, D. Zhou and Y. Huang, Photoactivatable prodrug-backboned polymeric nanoparticles for efficient light-controlled gene delivery and synergistic treatment of platinum-resistant ovarian cancer, *Nano Lett.*, 2020, **20**, 3039–3049.
- 143 S. Diring, D. O. Wang, C. Kim, M. Kondo, Y. Chen and S. Kitagawa, Kamei, K.-i.; Furukawa, S., Localized cell stimulation by nitric oxide using a photoactive porous coordination polymer platform, *Nat. Commun.*, 2013, **4**, 2684.
- 144 Z. Deng, N. Wang, Y. Liu, Z. Xu, Z. Wang, T.-C. Lau and G. Zhu, A Photocaged, Water-oxidizing, and nucleolus-targeted Pt(IV) complex with a distinct anticancer mechanism, *J. Am. Chem. Soc.*, 2020, **142**, 7803–7812.
- 145 J. Xu, Y. Kuang, R. Lv, P. Yang, C. Li, H. Bi, B. Liu, D. Yang, Y. Dai, S. Gai, F. He, B. Xing and J. Lin, Charge convertibility and near infrared photon co-enhanced cisplatin chemotherapy based on upconversion nanoplatform, *Biomaterials*, 2017, **130**, 42–55.
- 146 S. Li, R. Liu, X. Jiang, Y. Qiu, X. Song, G. Huang, N. Fu, L. Lin, J. Song, X. Chen and H. Yang, Near-infrared light-triggered sulfur dioxide gas therapy of cancer, *ACS Nano*, 2019, **13**, 2103–2113.
- 147 H. Wang, W. Miao, F. Wang and Y. Cheng, A self-assembled coumarin-anchored dendrimer for efficient gene delivery and light-responsive drug delivery, *Biomacromolecules*, 2018, **19**, 2194–2201.
- 148 S. He, K. Krippes, S. Ritz, Z. Chen, A. Best, H.-J. Butt, V. Mailänder and S. Wu, Ultralow-intensity near-infrared light induces drug delivery by upconverting nanoparticles, *Chem. Commun.*, 2015, **51**, 431–434.
- 149 H.-B. Cheng, B. Qiao, H. Li, J. Cao, Y. Luo, K. M. Kotraiah Swamy, J. Zhao, Z. Wang, J. Y. Lee, X.-J. Liang and J. Yoon, Protein-activatable diarylethene monomer as a smart trigger of noninvasive control over reversible generation of singlet oxygen: A facile, switchable, theranostic strategy for photodynamic-immunotherapy, *J. Am. Chem. Soc.*, 2021, **143**, 2413–2422.
- 150 R. Klajn, Spiropyran-based dynamic materials, *Chem. Soc. Rev.*, 2014, **43**, 148–184.
- 151 R.-L. Han, J.-H. Shi, Z.-J. Liu, Y.-F. Hou and Y. Wang, Near-infrared light-triggered hydrophobic-to-hydrophilic switch nanovalve for on-demand cancer therapy, *ACS Biomater. Sci. Eng.*, 2018, **4**, 3478–3486.
- 152 Y. Wang and D. S. Kohane, External triggering and triggered targeting strategies for drug delivery, *Nat. Rev. Mater.*, 2017, **2**, 17020.
- 153 M. Karimi, P. Sahandi Zangabad, A. Ghasemi, M. Amiri, M. Bahrami, H. Malekzad, H. Ghahramanzadeh Asl, Z. Mahdih, M. Bozorgomid, A. Ghasemi, M. R. Rahmani Taji Boyuk and M. R. Hamblin, Temperature-responsive smart nano-carriers for delivery of therapeutic agents: Applications and recent advances, *ACS Appl. Mater. Interfaces*, 2016, **8**, 21107–21133.
- 154 H. S. Jung, P. Verwilt, A. Sharma, J. Shin, J. L. Sessler and J. S. Kim, Organic molecule-based photothermal agents: An expanding photothermal therapy universe, *Chem. Soc. Rev.*, 2018, **47**, 2280–2297.
- 155 L. Huang, Y. Li, Y. Du, Y. Zhang, X. Wang, Y. Ding, X. Yang, F. Meng, J. Tu, L. Luo and C. Sun, Mild photothermal therapy potentiates anti-PD-L1 treatment for immunologically cold tumors *via* an all-in-one and all-in-control strategy, *Nat. Commun.*, 2019, **10**, 4871.
- 156 S.-i. Yokota, M. Kitahara and K. Nagata, Benzylidene lactam compound, KNK437, a novel inhibitor of acquisition of thermo-tolerance and heat shock protein induction in human colon carcinoma cells, *Cancer Res.*, 2000, **60**, 2942–2948.
- 157 L. R. Hirsch, R. J. Stafford, J. A. Bankson, S. R. Sershen, B. Rivera, R. E. Price, J. D. Hazle, N. J. Halas and J. L. West, Nanoshell-mediated near-infrared thermal therapy of tumors under magnetic resonance guidance, *Proc. Natl. Acad. Sci. U. S. A.*, 2003, **100**, 13549–13554.
- 158 J.-J. Hu, Y.-J. Cheng and X.-Z. Zhang, Recent advances in nanomaterials for enhanced photothermal therapy of tumors, *Nanoscale*, 2018, **10**, 22657–22672.
- 159 Y. Liu, P. Bhattarai, Z. Dai and X. Chen, Photothermal therapy and photoacoustic imaging *via* nanotheranostics in fighting cancer, *Chem. Soc. Rev.*, 2019, **48**, 2053–2108.
- 160 Q. Guan, L.-L. Zhou, Y.-A. Li, W.-Y. Li, S. Wang, C. Song and Y.-B. Dong, Nanoscale covalent organic framework for combinatorial antitumor photodynamic and photothermal therapy, *ACS Nano*, 2019, **13**, 13304–13316.
- 161 P. Chen, Y. Ma, Z. Zheng, C. Wu, Y. Wang and G. Liang, Facile syntheses of conjugated polymers for photothermal tumour therapy, *Nat. Commun.*, 2019, **10**, 1192.

- 162 H. Zhang, J. Chen, N. Li, R. Jiang, X.-M. Zhu and J. Wang, Au nanobottles with synthetically tunable overall and opening sizes for chemo-photothermal combined therapy, *ACS Appl. Mater. Interfaces*, 2019, **11**, 5353–5363.
- 163 R. S. Riley and E. S. Day, Gold nanoparticle-mediated photothermal therapy: Applications and opportunities for multimodal cancer treatment, *Wiley Interdiscip. Rev.: Nanomed. Nanobiotechnol.*, 2017, **9**, e1449.
- 164 K. Y. Choi, G. Liu, S. Lee and X. Chen, Theranostic nanoplatfoms for simultaneous cancer imaging and therapy: Current approaches and future perspectives, *Nanoscale*, 2012, **4**, 330–342.
- 165 S. Sun, J. Chen, K. Jiang, Z. Tang, Y. Wang, Z. Li, C. Liu, A. Wu and H. Lin, Ce6-Modified carbon dots for multimodal-imaging-guided and single-NIR-laser-triggered photothermal/photodynamic synergistic cancer therapy by reduced irradiation power, *ACS Appl. Mater. Interfaces*, 2019, **11**, 5791–5803.
- 166 Y. Li, Z. Miao, Z. Shang, Y. Cai, J. Cheng and X. Xu, A visible- and NIR-light responsive photothermal therapy agent by chirality-dependent  $\text{MoO}_3-x$  nanoparticles, *Adv. Funct. Mater.*, 2020, **30**, 1906311.
- 167 D. de Melo-Diogo, C. Pais-Silva, D. R. Dias, A. F. Moreira and I. J. Correia, Strategies to improve cancer photothermal therapy mediated by nanomaterials, *Adv. Healthcare Mater.*, 2017, **6**, 1700073.
- 168 F. Zhou, S. Wu, S. Song, W. R. Chen, D. E. Resasco and D. Xing, Antitumor immunologically modified carbon nanotubes for photothermal therapy, *Biomaterials*, 2012, **33**, 3235–3242.
- 169 L. Chen, L. Zhou, C. Wang, Y. Han, Y. Lu, J. Liu, X. Hu, T. Yao, Y. Lin, S. Liang, S. Shi and C. Dong, Tumor-targeted drug and CpG delivery system for phototherapy and docetaxel-enhanced immunotherapy with polarization toward M1-Type macrophages on triple negative breast cancers, *Adv. Sci.*, 2019, **31**, 1904997.
- 170 C. Zhang, Y. Yong, L. Song, X. Dong, X. Zhang, X. Liu, Z. Gu, Y. Zhao and Z. Hu, Multifunctional  $\text{WS}_2$ @Poly(ethylene imine) nanoplatfoms for imaging guided gene-photothermal synergistic therapy of cancer, *Adv. Healthcare Mater.*, 2016, **5**, 2776–2787.
- 171 H. Peng, J. Tang, R. Zheng, G. Guo, A. Dong, Y. Wang and W. Yang, Nuclear-targeted multifunctional magnetic nanoparticles for photothermal therapy, *Adv. Healthcare Mater.*, 2017, **6**, 1601289.
- 172 Y. Wang, Y. Song, G. Zhu, D. Zhang and X. Liu, Highly biocompatible BSA- $\text{MnO}_2$  nanoparticles as an efficient near-infrared photothermal agent for cancer therapy, *Chin. Chem. Lett.*, 2018, **29**, 1685–1688.
- 173 S. Liu, X. Pan and H. Liu, Two-dimensional nanomaterials for photothermal therapy, *Angew. Chem., Int. Ed.*, 2020, **59**, 5890–5900.
- 174 J. Shao, C. Ruan, H. Xie, Z. Li, H. Wang, P. K. Chu and X.-F. Yu, Black-phosphorus-incorporated hydrogel as a sprayable and biodegradable photothermal platform for postsurgical treatment of cancer, *Adv. Sci.*, 2018, **5**, 1700848.
- 175 C. Dai, S. Zhang, Z. Liu, R. Wu and Y. Chen, Two-dimensional graphene augments nanosensitized sonocatalytic tumor eradication, *ACS Nano*, 2017, **11**, 9467–9480.
- 176 H. Lin, Y. Wang, S. Gao, Y. Chen and J. Shi, Theranostic 2D tantalum carbide (MXene), *Adv. Mater.*, 2018, **30**, 1703284.
- 177 H. Lin, Y. Chen and J. Shi, Insights into 2D MXenes for versatile biomedical applications: Current advances and challenges ahead, *Adv. Sci.*, 2018, **5**, 1800518.
- 178 S. Wang, J. Shao, Z. Li, Q. Ren, X.-F. Yu and S. Liu, Black phosphorus-based multimodal nanoagent: Showing targeted combinatory therapeutics against cancer metastasis, *Nano Lett.*, 2019, **19**, 5587–5594.
- 179 Z. Wang, Y. Zou, Y. Li and Y. Cheng, Metal-containing polydopamine nanomaterials: Catalysis, energy, and theranostics, *Small*, 2020, **16**, 1907042.
- 180 H. Zhang, Y. Sun, R. Huang, H. Cang, Z. Cai and B. Sun, pH-sensitive prodrug conjugated polydopamine for NIR-triggered synergistic chemo-photothermal therapy, *Eur. J. Pharm. Biopharm.*, 2018, **128**, 260–271.
- 181 B. Poinard, S. Z. Y. Neo, E. L. L. Yeo, H. P. S. Heng, K. G. Neoh and J. C. Y. Kah, Polydopamine nanoparticles enhance drug release for combined photodynamic and photothermal therapy, *ACS Appl. Mater. Interfaces*, 2018, **10**, 21125–21136.
- 182 Y. Yang, X. Fan, L. Li, Y. Yang, A. Nuernisha, D. Xue, C. He, J. Qian, Q. Hu, H. Chen, J. Liu and W. Huang, Semiconducting polymer nanoparticles as theranostic system for near-infrared-II fluorescence imaging and photothermal therapy under safe laser fluence, *ACS Nano*, 2020, **14**, 2509–2521.
- 183 D.-W. Zheng, S. Hong, L. Xu, C.-X. Li, K. Li, S.-X. Cheng and X.-Z. Zhang, Hierarchical micro-/nanostructures from human hair for biomedical applications, *Adv. Mater.*, 2018, **30**, 1800836.
- 184 Z. Mi, P. Yang, R. Wang, J. Unruangsri, W. Yang, C. Wang and J. Guo, Stable radical cation-containing covalent organic frameworks exhibiting remarkable structure-enhanced photothermal conversion, *J. Am. Chem. Soc.*, 2019, **141**, 14433–14442.
- 185 B. Lü, Y. Chen, P. Li, B. Wang, K. Müllen and M. Yin, Stable radical anions generated from a porous perylene diimide metal-organic framework for boosting near-infrared photothermal conversion, *Nat. Commun.*, 2019, **10**, 767.
- 186 L. Wen, L. Chen, S. Zheng, J. Zeng, G. Duan, Y. Wang, G. Wang, Z. Chai, Z. Li and M. Gao, Ultrasmall biocompatible  $\text{WO}_3-x$  nanodots for multi-modality imaging and combined therapy of cancers, *Adv. Mater.*, 2016, **28**, 5072–5079.
- 187 K. Wen, L. Wu, X. Wu, Y. Lu, T. Duan, H. Ma, A. Peng, Q. Shi and H. Huang, Precisely tuning photothermal and photodynamic effects of polymeric nanoparticles by controlled copolymerization, *Angew. Chem., Int. Ed.*, 2020, **59**, 12756–12761.
- 188 J. Wang, X. Tan, X. Pang, L. Liu, F. Tan and N. Li,  $\text{MoS}_2$  quantum dot@polyaniline inorganic-organic nanohybrids for in vivo dual-modal imaging guided synergistic photothermal/radiation therapy, *ACS Appl. Mater. Interfaces*, 2016, **8**, 24331–24338.
- 189 S. Li, K. Gu, H. Wang, B. Xu, H. Li, X. Shi, Z. Huang and H. Liu, Degradable holey palladium nanosheets with

- highly active 1D nanoholes for synergetic phototherapy of hypoxic tumors, *J. Am. Chem. Soc.*, 2020, **142**, 5649–5656.
- 190 W. Li, J. Yang, L. Luo, M. Jiang, B. Qin, H. Yin, C. Zhu, X. Yuan, J. Zhang, Z. Luo, Y. Du, Q. Li, Y. Lou, Y. Qiu and J. You, Targeting photodynamic and photothermal therapy to the endoplasmic reticulum enhances immunogenic cancer cell death, *Nat. Commun.*, 2019, **10**, 3349.
- 191 L. Cheng, F. Zhang, S. Wang, X. Pan, S. Han, S. Liu, J. Ma, H. Wang, H. Shen, H. Liu and Q. Yuan, Activation of prodrugs by NIR-triggered release of exogenous enzymes for locoregional chemo-photothermal therapy, *Angew. Chem., Int. Ed.*, 2019, **58**, 7728–7732.
- 192 Q. Chen, L. Xu, C. Liang, C. Wang, R. Peng and Z. Liu, Photothermal therapy with immune-adjuvant nanoparticles together with checkpoint blockade for effective cancer immunotherapy, *Nat. Commun.*, 2016, **7**, 13193.
- 193 G. C. Li, N. F. Mivechi and G. Weitzel, Heat shock proteins, thermotolerance, and their relevance to clinical hyperthermia, *Int. J. Hyperthermia*, 1995, **11**, 459–488.
- 194 J. W. Fisher, S. Sarkar, C. F. Buchanan, C. S. Szot, J. Whitney, H. C. Hatcher, S. V. Torti, C. G. Rylander and M. N. Rylander, Photothermal response of human and murine cancer cells to multiwalled carbon nanotubes after laser irradiation, *Cancer Res.*, 2010, **70**, 9855–9864.
- 195 Y. Yang, W. Zhu, Z. Dong, Y. Chao, L. Xu, M. Chen and Z. Liu, 1D coordination polymer nanofibers for low-temperature photothermal therapy, *Adv. Mater.*, 2017, **29**, 1703588.
- 196 G. Gao, Y.-W. Jiang, W. Sun, Y. Guo, H.-R. Jia, X.-W. Yu, G.-Y. Pan and F.-G. Wu, Molecular targeting-mediated mild-temperature photothermal therapy with a smart albumin-based nanodrug, *Small*, 2019, **15**, 1900501.
- 197 F. Ding, X. Gao, X. Huang, H. Ge, M. Xie, J. Qian, J. Song, Y. Li, X. Zhu and C. Zhang, Polydopamine-coated nucleic acid nanogel for siRNA-mediated low-temperature photothermal therapy, *Biomaterials*, 2020, **245**, 119976.
- 198 G. Gao, Y.-W. Jiang, Y. Guo, H.-R. Jia, X. Cheng, Y. Deng, X.-W. Yu, Y.-X. Zhu, H.-Y. Guo, W. Sun, X. Liu, J. Zhao, S. Yang, Z.-W. Yu, F. M. S. Raya, G. Liang and F.-G. Wu, Enzyme-mediated tumor starvation and phototherapy enhance mild-temperature photothermal therapy, *Adv. Funct. Mater.*, 2020, **30**, 1909391.
- 199 Q.-W. Chen, X.-H. Liu, J.-X. Fan, S.-Y. Peng, J.-W. Wang, X.-N. Wang, C. Zhang, C.-J. Liu and X.-Z. Zhang, Self-mineralized photothermal bacteria hybridizing with mitochondria-targeted metal-organic frameworks for augmenting photothermal tumor therapy, *Adv. Funct. Mater.*, 2020, **30**, 1909806.
- 200 S. Shen, L. Feng, S. Qi, J. Cao, Y. Ge, L. Wu and S. Wang, Reversible thermochromic nanoparticles composed of a eutectic mixture for temperature-controlled photothermal therapy, *Nano Lett.*, 2020, **20**, 2137–2143.
- 201 J. Wu, D. H. Bremner, S. Niu, M. Shi, H. Wang, R. Tang and L.-M. Zhu, Chemodrug-gated biodegradable hollow mesoporous organosilica nanotheranostics for multimodal imaging-guided low-temperature photothermal therapy/chemotherapy of cancer, *ACS Appl. Mater. Interfaces*, 2018, **10**, 42115–42126.
- 202 Y. Lyu, J. Li and K. Pu, Second near-infrared absorbing agents for photoacoustic imaging and photothermal therapy, *Small Methods*, 2019, **3**, 1900553.
- 203 Y. Jiang, J. Huang, C. Xu and K. Pu, Activatable polymer nanoagonist for second near-infrared photothermal immunotherapy of cancer, *Nat. Commun.*, 2021, **12**, 742.
- 204 Q. Zhang, Q. Guo, Q. Chen, X. Zhao, S. J. Pennycook and H. Chen, Highly efficient 2D NIR-II photothermal agent with Fenton catalytic activity for cancer synergistic photothermal-chemodynamic therapy, *Adv. Sci.*, 2020, **7**, 1902576.
- 205 G. Liu, J. Zhu, H. Guo, A. Sun, P. Chen, L. Xi, W. Huang, X. Song and X. Dong, Mo<sub>2</sub>C-Derived polyoxometalate for NIR-II photoacoustic imaging-guided chemodynamic/photothermal synergistic therapy, *Angew. Chem., Int. Ed.*, 2019, **58**, 18641–18646.
- 206 C. Guo, H. Yu, B. Feng, W. Gao, M. Yan, Z. Zhang, Y. Li and S. Liu, Highly efficient ablation of metastatic breast cancer using ammonium-tungsten-bronze nanocube as a novel 1064 nm-laser-driven photothermal agent, *Biomaterials*, 2015, **52**, 407–416.
- 207 D. Xi, M. Xiao, J. Cao, L. Zhao, N. Xu, S. Long, J. Fan, K. Shao, W. Sun, X. Yan and X. Peng, NIR light-driving barrier-free group rotation in nanoparticles with an 88.3% photothermal conversion efficiency for photothermal therapy, *Adv. Mater.*, 2020, **32**, 1907855.
- 208 C. Bi, J. Chen, Y. Chen, Y. Song, A. Li, S. Li, Z. Mao, C. Gao, D. Wang, H. Möhwald and H. Xia, Realizing a record photothermal conversion efficiency of spiky gold nanoparticles in the second near-infrared window by structure-based rational design, *Chem. Mater.*, 2018, **30**, 2709–2718.
- 209 J. Zhou, Y. Jiang, S. Hou, P. K. Upputuri, D. Wu, J. Li, P. Wang, X. Zhen, M. Pramanik, K. Pu and H. Duan, Compact plasmonic blackbody for cancer theranosis in the near-infrared II window, *ACS Nano*, 2018, **12**, 2643–2651.
- 210 C. Liu, S. Zhang, J. Li, J. Wei, K. Müllen and M. Yin, A Water-Soluble, NIR-Absorbing quaterrylenediimide chromophore for photoacoustic imaging and efficient photothermal cancer therapy, *Angew. Chem., Int. Ed.*, 2019, **58**, 1638–1642.
- 211 Q. Zhan, X. Shi, J. Zhou, L. Zhou and S. Wei, Drug-controlled release based on complementary base pairing rules for photodynamic-photothermal synergistic tumor treatment, *Small*, 2019, **15**, 1803926.
- 212 M. D. Topal and J. R. Fresco, Complementary base pairing and the origin of substitution mutations, *Nature*, 1976, **263**, 285–289.
- 213 V. Bagalkot, O. C. Farokhzad, R. Langer and S. Jon, An aptamer-doxorubicin physical conjugate as a novel targeted drug-delivery platform, *Angew. Chem., Int. Ed.*, 2006, **45**, 8149–8152.
- 214 V. Raeesi, L. Y. T. Chou and W. C. W. Chan, Tuning the drug loading and release of DNA-assembled gold-nanorod superstructures, *Adv. Mater.*, 2016, **28**, 8511–8518.
- 215 L. He, C. Mao, M. Brasino, A. Harguindey, W. Park, A. P. Goodwin and J. N. Cha, TiO<sub>2</sub>-Capped gold nanorods for plasmon-enhanced production of reactive oxygen species and photothermal delivery of chemotherapeutic agents, *ACS Appl. Mater. Interfaces*, 2018, **10**, 27965–27971.

- 216 Y. Zhang, Z. Hou, Y. Ge, K. Deng, B. Liu, X. Li, Q. Li, Z. Cheng, P. A. Ma, C. Li and J. Lin, DNA-hybrid-gated photothermal mesoporous silica nanoparticles for NIR-responsive and aptamer-targeted drug delivery, *ACS Appl. Mater. Interfaces*, 2015, **7**, 20696–20706.
- 217 S. Huo, N. Gong, Y. Jiang, F. Chen, H. Guo, Y. Gan, Z. Wang, A. Herrmann and X.-J. Liang, Gold-DNA nanosunflowers for efficient gene silencing with controllable transformation, *Sci. Adv.*, 2019, **5**, eaaw6264.
- 218 E. M. McGuffie, D. Pacheco, G. M. R. Carbone and C. V. Catapano, Antigenic and antiproliferative effects of a *c-myc*-targeting phosphorothioate triple helix-forming oligonucleotide in human leukemia cells, *Cancer Res.*, 2000, **60**, 3790–3799.
- 219 R. Garzon and E. Al, MicroRNAs in cancer, *Annu. Rev. Med.*, 2009, **60**, 167–179.
- 220 M. M. Lino, S. Simões, A. Vilaça, H. Antunes, A. Zonari and L. Ferreira, Modulation of angiogenic activity by light-activatable miRNA-loaded nanocarriers, *ACS Nano*, 2018, **12**, 5207–5220.
- 221 R. S. Riley, M. N. Dang, M. M. Billingsley, B. Abraham, L. Gundlach and E. S. Day, Evaluating the mechanisms of light-triggered siRNA release from nanoshells for temporal control over gene regulation, *Nano Lett.*, 2018, **18**, 3565–3570.
- 222 H. Peng, C. Le, J. Wu, X.-F. Li, H. Zhang and X. C. Le, A genome-editing nanomachine constructed with a clustered regularly interspaced short palindromic repeats system and activated by near-infrared illumination, *ACS Nano*, 2020, **14**, 2817–2826.
- 223 J. Qiu, D. Huo, J. Xue, G. Zhu, H. Liu and Y. Xia, Encapsulation of a phase-change material in nanocapsules with a well-defined hole in the wall for the controlled release of drugs, *Angew. Chem., Int. Ed.*, 2019, **58**, 10606–10611.
- 224 Y. Yu, Y. Cheng, J. Tong, L. Zhang, Y. Wei and M. Tian, Recent advances in thermo-sensitive hydrogels for drug delivery, *J. Mater. Chem. B*, 2021, **9**, 2979–2992.
- 225 C. Zhu, D. Huo, Q. Chen, J. Xue, S. Shen and Y. Xia, A eutectic mixture of natural fatty acids can serve as the gating material for near-infrared-triggered drug release, *Adv. Mater.*, 2017, **29**, 1703702.
- 226 G. Liu, S. Zhang, Y. Shi, X. Huang, Y. Tang, P. Chen, W. Si, W. Huang and X. Dong, “Wax-Sealed” theranostic nanoplatform for enhanced afterglow imaging-guided photothermally triggered photodynamic therapy, *Adv. Funct. Mater.*, 2018, **28**, 1804317.
- 227 F. Doberenz, K. Zeng, C. Willems, K. Zhang and T. Groth, Thermoresponsive polymers and their biomedical application in tissue engineering – a review, *J. Mater. Chem. B*, 2020, **8**, 607–628.
- 228 Z. Wang, X. He, T. Yong, Y. Miao, C. Zhang and B. Zhong Tang, Multicolor tunable polymeric nanoparticle from the tetraphenylethylene cage for temperature sensing in living cells, *J. Am. Chem. Soc.*, 2020, **142**, 512–519.
- 229 M. S. Yavuz, Y. Cheng, J. Chen, C. M. Cobley, Q. Zhang, M. Rycenga, J. Xie, C. Kim, K. H. Song, A. G. Schwartz, L. V. Wang and Y. Xia, Gold nanocages covered by smart polymers for controlled release with near-infrared light, *Nat. Mater.*, 2009, **8**, 935–939.
- 230 Q. Zhang and R. Hoogenboom, Polymers with upper critical solution temperature behavior in alcohol/water solvent mixtures, *Prog. Polym. Sci.*, 2015, **48**, 122–142.
- 231 W. Hu, X. Bai, Y. Wang, Z. Lei, H. Luo and Z. Tong, Upper critical solution temperature polymer-grafted hollow mesoporous silica nanoparticles for near-infrared-irradiated drug release, *J. Mater. Chem. B*, 2019, **7**, 5789–5796.
- 232 X. Zhen, C. Xie, Y. Jiang, X. Ai, B. Xing and K. Pu, Semi-conducting photothermal nanoagonist for remote-controlled specific cancer therapy, *Nano Lett.*, 2018, **18**, 1498–1505.
- 233 P. Wang, L. Zhang, W. Zheng, L. Cong, Z. Guo, Y. Xie, L. Wang, R. Tang, Q. Feng, Y. Hamada, K. Gonda, Z. Hu, X. Wu and X. Jiang, Thermo-triggered release of CRISPR-Cas9 system by lipid-encapsulated gold nanoparticles for tumor therapy, *Angew. Chem., Int. Ed.*, 2018, **57**, 1491–1496.
- 234 A. Qu, X. Wu, S. Li, M. Sun, L. Xu, H. Kuang and C. Xu, An NIR-responsive DNA-mediated nanotetrahedron enhances the clearance of senescent cells, *Adv. Mater.*, 2020, **32**, 2000184.
- 235 B. Ouyang, F. Liu, S. Ruan, Y. Liu, H. Guo, Z. Cai, X. Yu, Z. Pang and S. Shen, Localized free radicals burst triggered by NIR-II Light for augmented low-temperature photothermal therapy, *ACS Appl. Mater. Interfaces*, 2019, **11**, 38555–38567.
- 236 R. Guo, Y. Tian, Y. Wang and W. Yang, Near-infrared laser-triggered nitric oxide nanogenerators for the reversal of multidrug resistance in cancer, *Adv. Funct. Mater.*, 2017, **27**, 1606398.
- 237 E.-Y. Chuang, C.-C. Lin, K.-J. Chen, D.-H. Wan, K.-J. Lin, Y.-C. Ho, P.-Y. Lin and H.-W. Sung, A FRET-guided, NIR-responsive bubble-generating liposomal system for *in vivo* targeted therapy with spatially and temporally precise controlled release, *Biomaterials*, 2016, **93**, 48–59.
- 238 Y. Ding, C. Du, J. Qian and C.-M. Dong, NIR-responsive polypeptide nanocomposite generates NO gas, mild photothermia, and chemotherapy to reverse multidrug-resistant cancer, *Nano Lett.*, 2019, **19**, 4362–4370.
- 239 Y. Liu, G. Shu, X. Li, H. Chen, B. Zhang, H. Pan, T. Li, X. Gong, H. Wang, X. Wu, Y. Dou and J. Chang, Human HSP70 promoter-based prussian blue nanotheranostics for thermo-controlled gene therapy and synergistic photothermal ablation, *Adv. Funct. Mater.*, 2018, **28**, 1802026.
- 240 X. Chen, Y. Chen, H. Xin, T. Wan and Y. Ping, Near-infrared optogenetic engineering of photothermal nanoCRISPR for programmable genome editing, *Proc. Natl. Acad. Sci. U. S. A.*, 2020, **117**, 2395–2405.
- 241 K. Villa and M. Pumera, Fuel-free light-driven micro/nanomachines: Artificial active matter mimicking nature, *Chem. Soc. Rev.*, 2019, **48**, 4966–4978.
- 242 M. Xuan, J. Shao, C. Gao, W. Wang, L. Dai and Q. He, Self-propelled nanomotors for thermomechanically percolating cell membranes, *Angew. Chem., Int. Ed.*, 2018, **57**, 12463–12467.
- 243 W. Wang, Z. Wu, X. Lin, T. Si and Q. He, Gold-nanoshell-functionalized polymer nanoswimmer for photomechanical poration of single-cell membrane, *J. Am. Chem. Soc.*, 2019, **141**, 6601–6608.

## Review

- 244 H. Xiong, X. Li, P. Kang, J. Perish, F. Neuhaus, J. E. Ploski, S. Kroener, M. O. Ogunyankin, J. E. Shin, J. A. Zasadzinski, H. Wang, P. A. Slesinger, A. Zumbuehl and Z. Qin, Near-infrared light triggered-release in deep brain regions using ultra-photosensitive nanovesicles, *Angew. Chem., Int. Ed.*, 2020, **59**, 8608–8615.
- 245 M. Wang, F. He, H. Li, S. Yang, J. Zhang, P. Ghosh, H.-H. Wang and Z. Nie, Near-infrared light-activated DNA-agonist nanodevice for nongenetically and remotely controlled cellular signaling and behaviors in live animals, *Nano Lett.*, 2019, **19**, 2603–2613.
- 246 S. Chen, A. Z. Weitemier, X. Zeng, L. He, X. Wang, Y. Tao, A. J. Y. Huang, Y. Hashimoto-dani, M. Kano, H. Iwasaki, L. K. Parajuli, S. Okabe, D. B. L. Teh, A. H. All, I. Tsutsui-Kimura, K. F. Tanaka, X. Liu and T. J. McHugh, Near-infrared deep brain stimulation *via* upconversion nanoparticle-mediated optogenetics, *Science*, 2018, **359**, 679–684.
- 247 Y. Ma, J. Bao, Y. Zhang, Z. Li, X. Zhou, C. Wan, L. Huang, Y. Zhao, G. Han and T. Xue, Mammalian near-infrared image vision through injectable and self-powered retinal nanoantennae, *Cell*, 2019, **177**, 243–255.